

BIOMECHANICS OF PROSTHETIC KNEE SYSTEMS: ROLE OF DAMPENING AND ENERGY
STORAGE SYSTEMS

HANDE ARGUNSAH BAYRAM



Bachelor of Industrial Engineering

Bahcesehir University, Turkey

June, 2005

Master of Technology

Kent State University

May, 2007

Submitted in partial fulfillment of requirement for the degree

DOCTOR OF ENGINEERING IN APPLIED BIOMEDICAL ENGINEERING

at the

CLEVELAND STATE UNIVERSITY

April, 2013

This dissertation has been approved
for the Department of Chemical and Biomedical Engineering
and the College of Graduate Studies by

Dissertation Committee Chairperson, Brian L. Davis, PhD
Department of Biomedical Engineering

Date

Nolan B. Holland, PhD
Department of Chemical and Biomedical Engineering

Date

Ahmet Erdemir, PhD
Department of Chemical and Biomedical Engineering

Date

George Chatzimavroudis, PhD
Department of Chemical and Biomedical Engineering

Date

Oya Icmeli Tukel, PhD
Department of Operations and Supply Chain Management

Date



To my precious son, Ege...

ACKNOWLEDGEMENTS

I would like to thank my advisor, Dr. Brian L. Davis, for guiding me in this challenging research project. I was really lucky to have him as an advisor because his support and knowledge made it possible for me to present this dissertation. I learned so much from him both professionally and personally. I would like to gratefully and sincerely acknowledge his mentorship during my doctoral education.

I would like to express my sincere thanks to my co-advisor Dr. Nolan B. Holland. He has been always very understanding and helpful. Also, I would like to thank Dr. Ahmet Erdemir of Cleveland Clinic deeply, who has helped and supported me tremendously. It will not be an understatement to say that this thesis was enhanced by his guidance. I acknowledge the other members of my thesis committee, Dr. George Chatzimavroudis and Dr. Oya Icmeli Tukul for their time and support. I gratefully acknowledge the support of State of Ohio, Department of Development and Third Frontier Commission, which provided funding in support of Rapid Rehabilitation and Return to Function for Amputee Soldiers project.

I thank Karl West and Dr. D. Geoffrey Vince for providing me the best possible facilities, and opportunities at Cleveland Clinic. I would like to thank Rebecca Laird and Darlene Montgomery in Applied Biomedical Program at Cleveland State University for their endless support and professional help over the years. I would like to thank Dr. Hanz Richter and Ron Davis in Mechanical Engineering department at Cleveland State University for their time and guidance.

I would like to express my deepest appreciation to my family for their unending love and support.

I would like to thank my newborn son, Mehmet Ege, for allowing me to work on my testing during my pregnancy.

Last but not least, I want to express my deepest love to my dear husband Bugrahan for his endless support, countless sacrifices and being there for me all the time.



BIOMECHANICS OF PROSTHETIC KNEE SYSTEMS: ROLE OF DAMPENING AND ENERGY
STORAGE SYSTEMS

HANDE ARGUNSAH BAYRAM

ABSTRACT

One significant drawback of the commercial passive and microprocessed prosthetic devices, the inability of delivering positive energy when needed, is due to the absence of the knee flexion during stance phase. Moreover, consequences such as circumduction and disturbed gait pattern take place due to the improper energy flow at the knee and the absence of the positive energy delivery during the swing phase.

Current generation powered design has solved these problems by delivering the needed energy with heavy battery demanding motors, which increase the mass of the device significantly. Hence, the gait quality of transfemoral amputees has not improved significantly in the last 50 years due to the inefficient energy flow distribution causing the patient to hike his/her pelvis, which leads to back pain in the long run. In this context, state-of-art prosthetics technology is trending toward creating energy regenerative devices, which are able to harvest/ return energy during ambulation by a spring mechanism, since a spring not only permits significant power demand reduction but also provides high power-to-weight ratio.

This study will examine the sagittal plane knee moment versus knee flexion angle properties robotically, clinically and theoretically to explore the functional stiffness

of a healthy knee as well as a prosthetic knee during the energy return and harvest phases of gait. With this intention, a prosthetic knee test method will be developed for investigating the torque-angle properties of the knee by iteratively modifying the hip trajectory until achieving the closest to healthy knee biomechanics by a 3-Degree of Freedom (DOF) Simulator.

This research reveals that constant spring stiffness is suboptimal to varying gait requirements for different types of activity, due to the variability of the power requirements of the knee caused by the passive, viscous and elastic characteristics and the activation dependent properties of the muscles. Exploring this variation is crucial for the design of transfemoral prosthetic devices that aim to mimic normal gait. This research will contribute to a better understanding of determination of the prosthetic knee design strategy; hence, by using modern computational tools, a prosthetic knee device could be simulated even before initiating the hardware design process.

TABLE OF CONTENTS

	Page
LIST OF TABLES	xi
LIST OF FIGURES	xii
CHAPTER I	14
INTRODUCTION	14
1.1. Background and Motivation	14
1.2. Objectives	17
1.3. Organization of the Document	18
CHAPTER II	21
RECENT DEVELOPMENTS IN ABOVE-KNEE PROSTHETICS AND THE IMPORTANCE OF ENERGY RECOVERY IN TRANSFEMORAL AMPUTEE GAIT.....	21
2.1 Introduction	21
2.2 Significance of Transfemoral Amputation as a Clinical Problem	22
2.3 Commercially Available Protheses	24
2.4 Emerging Prosthesis Designs	26
2.5 Discussion.....	34
CHAPTER III	38
ACTIVE FUNCTIONAL STIFFNESS OF THE KNEE JOINT DURING THE ACTIVITIES OF DAILY LIVING.....	38
3.1 Introduction	38
3.2 Methods	40

3.3	Results	43
3.4	Discussion.....	48
CHAPTER IV.....		51
MECHANICAL SIMULATION OF HIP JOINT DURING WALKING FOR EVALUATION OF PROSTHETIC KNEE FUNCTIONAL STIFFNESS.....		51
4.1	Introduction	51
4.2	Materials and Methods	54
4.3	Results	62
4.3.1	Ground Loading Iteration Results	62
4.4	Discussion.....	70
CHAPTER V		73
VERIFICATION OF THE ENERGY HARVESTABLE TRANSFEMORAL PROSTHETIC KNEE SPRING UNIT		73
5.1	Introduction	73
5.2	Methods	81
5.3	Conclusion	84
CHAPTER VI.....		86
CONCLUSIONS AND FUTURE WORK		86
6.1	Conclusions	86
6.2	Future Work.....	89
BIBLIOGRAPHY		90
APPENDIX		100

Appendix A	101
Test Circuit and Instrumentation	101
Appendix B	102
HPA Test Protocol	102
Appendix C	103
HPA Spring Alternatives and Test Results	103
Appendix D	105
Abbreviations	105

LIST OF TABLES

Table	Page
i: Spatio-temporal measures.....	40
ii: Averaged energy flow during the activities of daily living.....	45
iii: Functional stiffness during the activities of daily living.....	47
iv: Design Specifications.....	81
v: LHL 1250D 03 Spring Specifications.....	81

LIST OF FIGURES

Figure	Page
1: Knee Joint Power during Self-selected Walking Speed	34
2: Averaged power profiles at the knee joint	45
3: Knee joint peak energy return/harvest phase functional stiffness profiles.	47
4: Mauch SNS Knee hydraulic cylinder	55
5: The Rotating Dial on the Hydraulic Unit	56
6: Össur Flex Foot.....	57
7: Complete Simulator Assembly.....	58
8: Illustration of the GRF iteration variables.....	59
9: Healthy Human Normal Walking Vertical GRF Profile	60
10: Mauch Microlite S Knee GRF Iteration I	62
11: Mauch Microlite S Knee GRF Iteration II	63
12: Hip angle trajectory iteration	64
13: Mauch Microlite S Knee GRF Iteration III	64
14: Mauch Microlite S Knee GRF Iteration IV	65
15: Mauch Microlite S Knee GRF Iteration V	66
16: Mauch Microlite S Knee GRF Iteration V	66
17: Healthy Knee Joint Normal Walking Biomechanics	68
18: Healthy Knee Joint Normal Walking Functional Stiffness.....	69
19: Mauch Microlite S Knee Normal Walking Functional Stiffness	69

20: Mauch Microlite S Knee Functional Stiffness	70
21: Symmetry of Gait during Normal Walking.....	71
22: Cleveland Clinic Foundation Knee hydraulic system	74
23: Schematics of the HPA and the Energy Storage Unit and HPA Components.....	75
24: Rotary Actuator Schematics	77
25: Slow, Normal and Fast (125.3±11.8 steps/min) cadences of the healthy knee joint:	79
26: Maximum pressure at the knee joint	82
27: Verification Test Results of the HPA	83
28: The High Pressure Accumulator and the caliper positioning	83
29: Validation Test Results of the HPA	84

CHAPTER I

INTRODUCTION

1.1. Background and Motivation

There are more than 300,000 transfemoral amputees in the United States (Adams, 1999) and every year 30,000 new transfemoral amputations occur (Feinglass, 1999). Diabetes and vascular diseases are the foremost causes of transtibial and transfemoral amputations by constituting the 33% and 59% of the overall cases respectively. The remaining 8% of the incidents are due to tumor, trauma, infection, and failed knee replacements. The ratio of transtibial amputation to transfemoral amputation cases is 3.5:1 (Allcock, 2001). Without effective intervention of the growth of diabetes, vascular diseases and their complications, there is an unfortunately high potential for the incidence to increase. This enhances the importance of developing prosthetic devices capable of providing near normal ambulation to amputee patients.

Besides the emotional and physical consequences, management of amputation is a high-priced treatment. Direct cost of lower extremity amputation ranges from \$20,000 to \$60,000 depending on the degree of the amputation (e.g. toe amputation vs.

transfemoral amputation) (National Institutes of Health, 2009). Along with the amputation surgery and associated hospitalization costs, amputees need prosthetic devices to achieve a certain degree of mobility. According to the conversations with the prosthetic knee companies, accouterment costs range from a few thousand dollars for the passive models (Mauch Knee: \$5,200, (Össur, Iceland)), about \$25,000 for microprocessed models (Plie MPC: \$18,475 (Freedom Innovations, CA, USA), C-leg: \$20,000, (Otto Bock, Germany), Rheo Knee: \$30,000, (Össur, Iceland)) and \$100,000 for the powered models (Power Knee: \$100,000, (Össur, Iceland)).

Ambroise Paré, a sixteenth century French army surgeon, is considered as the inventor of transfemoral prosthesis (Ham, 1991). This particular prosthesis was a pure mechanical device, which allowed kneeling and featured some other properties still used today such as knee lock mechanism and user-adjustable harness (Vitali, 1987). Currently, prosthetics technology has come a long way compared to Paré's mechanical device by using hydraulic, pneumatic and electrical/computer controlled elements in order to minimize the consequences of passive mechanisms (Zissimopoulos, 2007; Struyf, 2009; Kuo, 2007). Nevertheless, with the exception of Össur's Power Knee (Össur, Iceland), despite the increasing sophistication of prosthetic knee technology, the majority of the prostheses are controlled damping systems, which replicate the negative work functions of a biological knee, but cannot contribute positive work to gait (Martinez- Villalpando, 2009).

The emerging prosthetic knee designs (Gailey, 2008; Modan, 1998; Martinez- Villalpando, 2009; Sup, 2008; van den Bogert, 2012) elaborate the importance of efficient energy flow at the knee joint by harvesting/returning energy in a spring. A spring not only

permits significant power demand reduction by providing energy storage capacity but also allows high power-to-weight ratio (Argunsah and Davis, 2011). Therefore, instead of using heavy motors, gearboxes and bulky batteries, a spring can help the peak power demand of the prosthesis, by producing the needed positive energy during the stance phase with less weight.

In this work, the significance of energy flow in transfemoral amputee gait was explored along with recent developments, which emphasize harvesting/ returning energy in a spring by compressing/releasing it controllably during gait. However, constant spring stiffness is suboptimal to varying gait requirements for different types of daily activity, due to the variability of the impedance (Pfeifer, 2011), functional stiffness and the power requirements of the knee caused by the passive characteristics, viscous and elastic attributes and the activation dependent properties of the muscles in the joint (Johns, 1962; Winters, 1988). As it is not realistic to replace the energy storage element of the prosthesis for each performed activity, the efficiency of the spring should be supplemented by smart systems such as microprocessors, valves, pumps, motors etc. through adjusting the amount and timing of the spring compression/release depending on the biomechanical demands of the performed activity.

Nonetheless, for more efficient prosthetic knee design process, mimicking of the healthy human knee functional stiffness is necessary for providing the desirable quantitative values for loading and unloading intervals, which match the biomechanical demands of the performed activity to the best extent possible. This study examined sagittal plane knee moment versus knee flexion angle curves from 12 able-bodied

subjects during the activities of daily living with the aim of exploring the active knee joint functional stiffness. The slopes of the knee flexion moment versus knee flexion angle curves during walking at variable cadence, slow running, stair ascent/descent and sit/stand/ sit sequence were calculated to obtain the favorable active knee joint functional stiffness during the peak energy return (unloading) and energy harvest (loading) phases. With the same intention, a 3DOF prosthetic knee-testing robot was simulated the hip joint movement of purely passive Mauch Knee during normal walking for evaluating the knee functional stiffness and the importance of knee joint dampening. The use of the robot provided more controlled and consistent data by delivering the same conditions during each iteration. Therefore factors, which might cause inconsistency, such as patient variability, prosthetic knee familiarity and acclimation process, were eliminated from the Mauch Knee-healthy knee joint comparison in terms of knee joint functional stiffness analysis.

1.2. Objectives

The objectives of this thesis are four-fold:

- Investigate the significance of energy flow at the knee joint. This entails quantifying storage and release of energy at various phases of the gait cycle.
- Assess active knee joint functional stiffness during slow/normal/fast walking, slow running, stair ascent/descent and sit/stand/sit sequence. The desirable loading and unloading torsional spring stiffness rates were calculated to guide the prosthetic knee developers during the design strategy determination period; so

that, a prosthetic knee device could be simulated even before initiating the hardware design process.

- Analyze the functional stiffness of a purely passive prosthetic knee and compare with the healthy knee joint. This phase also identified potential shortcomings of passive designs in terms of possible requirements for mechanisms to provide positive energy to the system
- Finally, an energy storage unit mechanism, which is capable of harvesting and returning the required energy during the cyclic activities of daily living without utilizing a motor, was proposed for designing energy flow efficient microprocessed prosthetic knee devices.

The design goal of this work was to reproduce the hip kinematics and achieve the closest ambulation to a healthy knee with the 3DOF robot during normal walking with the purpose of eliminating the human factors from the data collection process. During the closest to normal ambulation conditions, the importance of dampening and the need for an energy storage/ release and/or production mechanism were presented.

1.3. Organization of the Document

This dissertation is organized in five chapters. Chapter I presents the motivation of this work and emphasizes the requirement of examining the knee joint functional stiffness of the healthy knee joint as well as a purely passive prosthetic knee in order to explore the energy flow at the knee joint and highlights the importance of using an energy harvest/ return element in prosthetic knee designs.

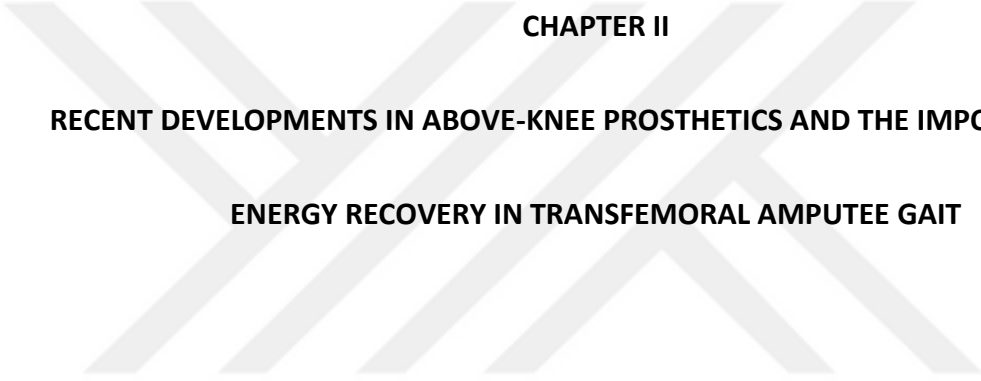
Chapter II is a literature review, describing the commercial prostheses, their limitations and the state-of-art trends in achieving assisted gait by harvesting/ returning energy in a controlled manner by using a spring unit (Unal, 2011; Demšar, 2011; Farber, 1995; Sup, 2008; Martinez- Villalpando; 2009, van den Bogert, 2012). The idea of using a spring is based on helping the peak power demand of the prosthesis during the stance phase of gait. Ideally, during this phase, a spring should store energy and release the appropriate amount when the knee joint requires positive energy during the swing phase.

Chapter III explores the broad-based data set covering the flow of energy at the knee joint for a range of subjects over a wide variety of conditions. The energy harvest/ return phases and the required functional spring stiffness are identified during those periods of the gait cycle when efficiency needed to be increased. The variability in obtained stiffness rates across the activities of daily living gives some indication of the difficulty of achieving high efficiency in a simple passive mechanism, which challenges the designers' ingenuity. Therefore, rather than using heavy motors, which increase the power demand of the mechanism, a spring would deliver the needed positive energy back to the system when it is supported by smart arrangements such as series-elastic actuators (Martinez-Villalpando, 2009) and/or valve operated spring loaded hydraulic accumulators (van den Bogert, 2012).

Chapter IV presents the functional stiffness analysis of a purely passive prosthetic knee during mechanically simulated normal walking. The Mauch Microlite S Knee was loaded by a 3DOF Prosthetic Knee Testing Robot system, which was designed and assembled at the Cleveland State University. The kinematics of the hip and the ground reaction forces

(GRF) during the stance phase were reproduced by the robot through an iterative process with the aim of obtaining a natural gait pattern. For the desirable GRF condition, the functional stiffness of the Mauch Knee was calculated and the associated knee joint movement was compared with the healthy knee in terms of gait symmetry. Therefore, the major drawback of the passive prosthetic devices, the lack of positive energy delivery when needed due to the absence of an energy storage component and/or electrically controlled mechanisms, was verified and the importance of the efficient energy flow at the knee joint and the importance of dampening were emphasized.

Chapter V represents the verification test results of a newly proposed, controlled passive variable-damping above-knee prosthesis prototype energy storage mechanism. The obtained results indicated that, during the cyclic activities of daily living, an energy storage mechanism, when it is supplemented by smart mechanisms that include valves and microprocessors, the required energy can be harvested and returned back to the system in order to provide assisted gait to the patient without utilizing heavy motors in the system.



CHAPTER II

RECENT DEVELOPMENTS IN ABOVE-KNEE PROSTHETICS AND THE IMPORTANCE OF

ENERGY RECOVERY IN TRANSFEMORAL AMPUTEE GAIT

2.1 Introduction

Above knee amputations occur for a variety of reasons such as disease, tumor, trauma, infection, or failed knee replacements. According to the National Limb Loss Information Center’s statistics, in 2007 amputations due to vascular disease accounted for the majority (82 percent) of limb loss discharges. This rate increased from 38.30 per 100,000 people in 1988 to 46.19 per 100,000 people in 1996. War related trauma and accidents constitute the remaining 18%. It has been reported that 266,465 people had a transfemoral amputation between 1988 and 1996 and more than 80% of the amputations were due to diabetes, which is described as a new epidemic, with the number of diagnosed adults tripling between 1980 and 2005. According to the statistics, one third of Americans are expected to be diabetic by 2050 (US center of disease, 2011; Centers for

Disease Control and Prevention, 2011). Without effective intervention of the growth of diabetes and treatment of its complications, this number has an unfortunate high potential to grow. The prevention of death from diabetic complications may result in more amputees eventually experiencing serious, non-fatal consequences; making them even more sedentary via inadequate prostheses use, which not only reduces their quality of life but also accelerates other metabolic and cardiovascular problems.

Besides the emotional and physical consequences of lower limb amputation, the direct cost of lower extremity amputation ranges from \$20,000 to \$60,000 depending on the degree of the amputation (e.g. toe amputation vs. transfemoral amputation). Along with the amputation surgery and the hospitalization costs, the amputee needs to achieve a certain degree of mobility. Selection of the prosthetic is done after considering various patient factors such as age, weight, reason and level of amputation, other health conditions and amputee motivation. According to prosthetic knee manufacturers, for a basic prosthesis, costs range from a few thousand dollars for the passive models, about \$20,000 for microprocessed models and \$100,000 for the powered models.

2.2 Significance of Transfemoral Amputation as a Clinical Problem

The prosthetic knee market provides the amputee with many choices including purely passive, hydraulic, pneumatic, friction-based and powered models. Current generation prostheses, except the purely passive models, are supplemented by microprocessors and a variety of sensor techniques such as electromyography, knee angle sensors, heel strike/toe off indication switches and foot load cells. Nevertheless, the gait quality of

transfemoral amputees has not improved significantly in the last 50 years due to the inefficient knee joint energy flow distribution of the commercial prosthetic knees along with the absence of the proper knee flexion during the swing phase, causing the patient to hike his/her pelvis, which leads to back pain in the long run. In this context, state-of-art prosthetics technology is trending toward creating energy regenerative devices, which are able to harvest and return metabolic energy during ambulation. The purpose of this present review is to identify the cons and pros of both the commercial prosthetic knees and the emerging designs, as well as to discuss the importance of energy flow at the knee joint by harvesting and returning energy in a controlled way.

Transfemoral amputation is one of the most traumatic medical treatments a patient can receive. Amputees not only lose physical function and neural feedback after amputation, but also have altered knee kinematics during the swing phase of the prosthetic limb, which causes abnormal pelvic movements in the frontal plane even with the most sophisticated microprocessed prosthetic knee available on the market today (Kulkarni, 2005; Gailey, 2008; Modan, 1998). In order to minimize the metabolic energy expenditure and reduce the need of muscular recompense of a transfemoral amputee, the overall energy distribution during the stance and swing phases should be balanced appropriately by the prosthesis to provide close to normal ambulation and minimize the aforementioned limitations.

2.3 Commercially Available Prostheses

Prosthetic knees on the market are classified into three groups: passive, microprocessed and powered. Passive prostheses do not comprise control and/or sensor units to manipulate the phases of gait, therefore they are unable sensing the knee angle and/or applied ground reaction force and responding accordingly. They provide ambulation by using their purely passive and not-computerized mechanisms, which cause not only flaws during swing phase but also incremental net metabolic energy consumption during the activities of daily living (Johansson, 2005).

Passive knees are able to accommodate walking on even surfaces at various cadences without providing the required positive energy back to the system. However, they are not capable of providing successful ambulation on uneven surfaces and during the positive energy dependent activities, such as sitting down/standing up and stair ascent/ descent (Kahle, 2008). Consequently, the patient is constrained to perform these activities with a step-by-step technique where the loading is applied on the healthy leg while the prosthetic limb follows it passively.

By incorporating software algorithms, microprocessed prosthetic knees are able to provide more efficient ambulation on uneven surfaces and during the activities of daily living compared to the passive models (Johansson, 2005; Chin, 2006). Microprocessed prosthetic knees provide more natural walking than the passive designs by improving the gait smoothness, reducing the overall work at the hip joint and the peak hip power generation at toe-off during controlled walking speeds. When they are compared with the passive knees at self-selected walking cadence, no significant difference in energy

consumption was observed (Marks, 1999; Johansson 2005; Kirker 1996; Buckley, 1997). In another study, Schmalz et al. (2002) presented that C-Leg has a minor advantage over the Mauch SNS at self-selected walking speed. Similarly, in Johansson et al.'s findings (2005), the energy consumption of Rheo Knee was 5% lower than Mauch SNS and 3% lower than the C-leg at self-selected walking speed.

Unlike the situation with a natural leg, where energy can be stored in tendons, neither passive nor microprocessed prostheses can store and release energy at a chosen time, to help propel the patient's forward motion by providing the required positive energy. They can only simulate joint resistance and damping, meaning that the truly natural motion of the leg is limited.

Powered prosthetic knees are composed of miniaturized motors, which require an electrical power source, to mimic muscle contractions and provide the required positive energy during ambulation. However, they are heavy (Power Knee weighs 4700 g, whereas the average weight of the commercial microprocessed knees is 1250 g) and relatively more expensive (Power Knee costs \$100,000 whereas, the average cost of the commercial microprocessed knees is \$20,000). Power Knee is the first and only active commercial prosthetic knee, which is capable of providing the needed positive energy, on the market (Dunne, 2010). By using the orthesis- Artificial Proprioception Module (APM) coupling, it communicates with the functional leg of the amputee, and mimics its movement. The orthesis sensor unit is worn on the intact leg and collects the real time data. The APM, located on the ankle of the Power Knee, receives the instantaneous data from the orthesis and sends them to the microprocessor. It is a rarely used prosthesis since it has not been

given a Medicare insurance reimbursement code due to its high price and reports on its performance are scarce in the literature. Currently only two veterans are using the Power Knee (Dunne, 2010). Besides its significantly high weight, it can only be used by the unilateral transfemoral amputees as the APM needs the real time data collected by the orthosis. Among the people who live with limb loss, the fraction of bilateral transfemoral amputees is approximately 18 percent (Stewart, 1993). In addition to the significantly high market price drawback of Power Knee, when the dramatically increasing obesity and diabetes rates are considered, it is anticipated that the number of bilateral transfemoral amputation will increase, that will reduce the number of potential Power Knee users.

2.4 Emerging Prosthesis Designs

2.4.1 Producing Positive Power

One significant drawback of the commercial passive and microprocessed prosthetic devices, the inability of delivering positive energy when needed, is due to the absence of the knee flexion during stance phase. Moreover, consequences such as circumduction and disturbed gait pattern take place due to the improper energy flow at the knee joint and the absence of the positive energy delivery during the swing phase. Current generation powered design has solved these problems by delivering the needed energy with heavy battery demanding motors, which increase the mass of the device significantly, whereas, it needs to be relatively less than the mass of the missing portion of the natural leg. Patients want a knee prosthetic device that is lightweight, quiet, and capable of delivering close to normal ambulation. The combination of these three

features in prosthetic limbs has proven to be difficult to provide. Patients want the prosthesis to be similar to the normal leg, including normal knee and ankle flexion angles during the activities of daily living (Aeyels, 1992). Thus, the prosthetic knee developers sought new methods to design efficient mechanisms, which are lightweight and at the same time energy regenerative.

A new approach utilizing spring mechanisms for improving energy efficiency during gait is gaining traction (Sup, 2008; Martinez-Villalpando, 2009; van den Bogert, 2012). Since gait is a cyclical pattern that has positive and negative work phases, using a spring can cut the power demand significantly by mimicking the musculotendonous structures by harvesting and returning the needed energy. A significant advantage of the spring is its high efficiency and high power-to-weight ratio (Argunsah and Davis, 2011). Instead of using heavy motors, gearboxes and bulky batteries, a spring can help the peak power demand of the prosthesis during the stance phase of gait with less weight.

Unal et al. (2010) at the University of Twente, The Netherlands, developed a completely passive transfemoral prosthetic knee prototype, which is capable of harvesting and returning energy by using a set of springs, coupling knee and ankle joints. The design of this knee is based on the balanced energy distribution in the ankle and knee joints during a single stride. The ankle joint behaves as an energy generator during the pre-swing phase and stores 80% of the required energy (Unal et al. 2010). During walking, the amount of the generated energy by the knee joint at the stance flexion phase and by the ankle joint at the early swing phase are stored in the spring couplings in order to provide the required energy to the knee joint during early swing and swing phases and to

the ankle joint during the early stance phase. Stance and swing phase performance was simulated separately. The results indicated that the prototype was able to store 76% of the required energy in the spring sets and distribute it to the knee and ankle joints throughout the stride by compressing, locking and releasing the springs according to the applied body weight. However, this design is not capable of producing ankle push-off force, as it is neither controlled nor powered. Therefore, for achieving near normal walking during other activities, which require more energy than walking, hybrid designs, which unite the passive mechanisms with smart control algorithms, are needed.

SymBiotechs XT9 (SymBiotechs, UT, USA) is another commercial passive prosthesis, which uses a spring mechanism to mimic the functions of the quadriceps during high activity sports by compressing the spring pneumatically depending on the applied force. However, it is not designed for normal daily use. Emerging designs take the advantage of using the high efficiency of a spring unit not only in storing and releasing energy during gait, but also in developing light, less expensive and energy regenerative prostheses, which are able to harvest energy from the movement of the user and instead of releasing the harvested energy immediately, would keep it until the energy is most needed during the swing phase.

2.4.2 Prostheses Mimicking Muscles

Massachusetts Institute of Technology (MIT), Vanderbilt University and Cleveland Clinic Foundation proposed transfemoral prosthetic device designs recently. Even though none of them have been commercialized, the common characteristic of these designs is the use

of a spring element to efficiently manipulate the energy distribution throughout the gait cycle and obtain close-to-normal ambulation via energy regeneration by harvesting energy from the gait and returning it at critical times, to minimize the size and weight of the drive systems and power supplies that assist knee rotation.

The MIT team proposed a powered knee prosthesis with two series-elastic actuators and spring elements positioned in parallel in an agonist-antagonist arrangement (Martinez-Villalpando, 2009). Stance and swing phases are controlled by two actuators, which are composed of series of springs, transmissions and torque sources. Stance phase is manipulated by compressing the extension and flexion springs. The flexion and extension motors keep the springs locked in order to store energy and unlocked in order to release it when needed.

Stance and swing phase stability is controlled by dividing the gait cycle into five phases. Stance phase is divided into three and swing phase is divided into two sub-phases, based on loading and knee angle dynamics of reference able-bodied human gait. During the heel strike phase, the extension spring is compressed as the amputee applies weight on the prosthesis. With that intention, the energy required to manipulate the stance extension phase is stored in the extension spring. During the stance extension phase, knee angle reaches the maximum extension, and returns the energy stored in the extension spring by releasing it and this energy is transferred to the flexion spring as the knee prepares to flex at the end of the stance phase. The compressed flexion spring causes the knee angle to reach the maximum knee flexion ($\sim 60^\circ$) and releases the stored energy.

During the stance phase, motors are used only for keeping the springs compressed to keep the stored energy as the prosthetic knee design also benefits from the gravity and the moment of inertia during the stance phase to minimize the power consumption. Conversely, during the swing phase, required damping is obtained by activating the springs electrically. Therefore, during the stance phase the motors are engaged as the supplements of the mechanical systems. Conversely, during the swing phase, mechanical systems become the supplementary element of the electrical components.

The human tests indicated that the knee torque, knee angle and power of the amputee match corresponding measures for the non-amputee subject. Moreover, the prosthetic knee was satisfactory in providing near-normal walking at self-selected walking speed on an even-surface by storing positive energy throughout the stance flexion phase to produce natural movement during push off (Martinez-Villalpando, 2009).

Conversely, it has been tested only at self-selected walking speed, where the power requirement is at minimum level. Additionally, it has been reported that for walking at variable speed, the springs on the flexion and extension axes need to be replaced with softer and stiffer springs respectively in order to provide the required knee stiffness to the amputee. Likewise, for the activities other than walking at self-selected speed, using linear springs on the axes would not be an option to any further extent, such that they need to be replaced by non-linear springs, which makes the control more complicated.

The Cleveland Clinic Foundation team proposed a microprocessed prosthesis, which is capable of harvesting/ returning energy in a controlled way (van den Bogert et al., 2012). Its hydraulic mechanism is composed of a linear actuator, two accumulators and

two valves. The linear actuator converts pressure to torque and torque to pressure. During stance phase, as the patient weight creates pressure, hydraulic flow is initiated through the high-pressure accumulator to obtain the required stiffness. When the applied weight starts to decrease, the accumulator pressure is routed back to the actuator to apply torque, which is needed to flex the knee. The high and low pressure valves open and close depending on the phase of the gait cycle to permit high pressure flow from/to the actuator. The high-pressure accumulator provides energy storage and release, while the low pressure accumulator houses the hydraulic fluid in the system. The electrical/electronic system includes the microprocessor, knee angle and leg force sensors.

At the beginning of the stance phase, body weight acts on the leg and starts flexing the knee. With the high-pressure chamber of the actuator connected to the high-pressure accumulator, this torque pumps the fluid into the high-pressure accumulator, which houses the energy storage unit. As the pressure is applied, a spring is compressed and energy is harvested. Once the available energy has been stored, the control valve of the high-pressure accumulator closes and holds the pressurized fluid in the accumulator. Modulating the orifice size of the low-pressure valve maintains the desired pressure/knee torque. In late stance/early swing phases, it is closed and the high-pressure valve is opened to produce the needed torque in the actuator to initiate the knee flexion. Only optimal control simulation results during walking, running and sit/stand/sit sequence are available in the literature, showing that the proposed device provided near normal knee

movement and stance phase flexion when the accumulator stiffness was adjusted to each tested activity (van den Bogert et al., 2012).

2.4.3 A New Approach: Union of Ankle and Knee Joints

Goldfarb team (2008) in Vanderbilt University proposed a powered knee and ankle prosthesis, which is powered pneumatically and capable of doing impedance control by using the feedback coming from its on-board sensors. The prosthesis is composed of two axes, on which knee and ankle actuators are located. The two servo valves, according to the feedback coming from the knee and ankle load cells, alter the stiffness of the actuators. A spring unit on the ankle control axis provides the knee flexion during early stance, therefore it not only reduces the energy required to flex the knee during the swing phase but also stores the available energy.

Stance and swing phase stabilities are controlled by dividing the gait cycle into four phases: stance flexion, pre-swing, swing flexion and swing extension. Within the gait phases, actuators are kept inactive to maintain the constant stiffness and in between the gait phases, the stiffness is changed dynamically in order to provide the required stiffness in the knee and ankle axes depending on the biomechanical demands of each particular gait phase.

Vanderbilt University's knee is the only transfemoral knee, which unites the knee and ankle joints in one mechanism to produce the required positive energy. The powered-tethered prototype was attached to an adult male able-bodied subject via a bent-knee adaptor. The subject was asked to walk on a treadmill at three controlled walking speeds

(2.2, 2.8 and 3.4 km/hr.) (Sup, 2008). An external 2.2 MPa pressure source along with a computer were used to operate it during testing. The behavior of the prototype between and within the four gait phase modes have been analyzed and compared with able-bodied human gait (Sup, 2008; Varol, 2008). The results showed that the prototype was able to manipulate the subjects' gait satisfactorily by producing three positive power peaks during the stance phase. However, due to its design constraints, the ankle actuator is capable of providing 76 percent of the maximum torque during the stance flexion phase since in order to maintain the weight of the prototype within the desired range, the team aimed to limit the maximum weight of the battery unit to 600-700 g. With that battery capacity 4.4-5 km of walking range could be obtained at self-selected cadence. Klute et al. (2006) reported the daily average step number of transfemoral amputees wearing C-leg as 2657 ± 737 . The average step length of a trained C-leg user is reported as $0.72\text{m} \pm 0.07$ (Segal, 2006), hence the distance that a trained C-leg user walks per day is approximately 4 km. Therefore, the proposed design almost reaches the limits of C-leg in terms of the delivered ambulation distance.

The emerging designs are breakthroughs when they are compared to the current generation prostheses by storing energy in a spring during early stance and returning it in late stance, but these current designs are effective over a limited range of conditions and are usually directed at a narrow sports activity (Sup, 2008; Martinez-Villalpando, 2009). A regenerative prosthesis could be a significant step forward with respect to improving the average activity level achieved by transfemoral amputees.

2.5 Discussion

A handicap with respect to designing new prostheses is a lack of broad-based data set covering energy flows at the knee and ankle joints for a range of subjects over a range of conditions. The margin of “negative” work at the knee over the “positive” work determines the required efficiency if the prosthesis is to be wholly regenerative. The match between the input and output impedances gives some indication of the difficulty of achieving high efficiency in a simple mechanism.

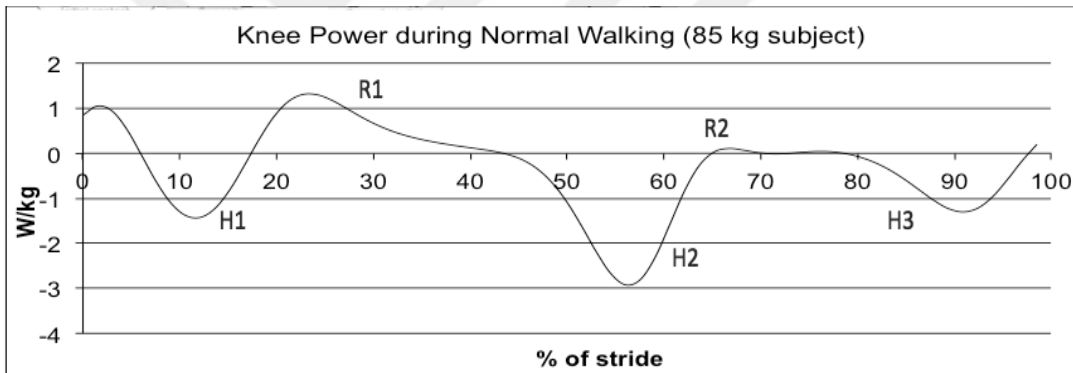


Figure 1: Knee Joint Power during Self-selected Walking Speed- The positive power peaks, indicating energy generation by muscles (R1 and R2); and negative power peaks, indicating energy harvest by muscles (H1, H2 and H3) of an able-bodied human at self-selected walking speed. Note that muscles act as a brake more than half of the time, which requires effective energy flow at the knee joint for a smooth and close to normal ambulation. At a glance, storing energy in the spring during H1 phase and releasing it immediately during the R1 phase, where energy is generated might seem to be the right solution to fix the energy flow deficiency at the knee joint. However, for the H2 phase, releasing all of the stored energy during R1 phase would be disadvantageous since this may cause toe to stub the ground right after the H2 phase because the energy at R2 is actually produced by the ankle joint and transfemoral amputees cannot generate H2 as able-bodied people because of the absence of an ankle joint.

Equally importantly, stiffness of the energy storage element for not only a wide range of activities but also during each sub-phase of gait cycle should be analyzed for ankle and

knee joints. Stiffness of the healthy ankle joint during walking at variable cadence has been investigated by Hansen et al (2004) with the purpose of guiding the designers in developing ankle joints which are capable of optimizing the energy flow and providing a near-normal ambulation. This study focused on the torque vs. ankle angle during loading and unloading conditions. The area between the hysteresis curves during walking at self-selected speed was almost zero, however, for controlled speed walking, larger hysteresis areas were obtained. This confirms that as the magnitude of the positive energy demand increases, the supplementary mechanisms, which control the spring compression/release become more crucial as for the activities such as walking at controlled speed, stair ascent/descent, sit/stand/sit sequence and running, purely passive mechanisms require the support of high-level arrangements such as series-elastic actuators (Martinez-Villalpando, 2009) and valve operated spring loaded hydraulic accumulators (van den Bogert, 2012). The normal gait during any activity of daily living is a combination of different body segments' motion with the purpose of translating the body with minimized energy cost (Alexander 2002). Human locomotion is a complex process, involving the interaction of many muscle groups and sensory systems. Traditionally, researchers consider six determinants of gait: (1) Pelvic rotation (lateral rotation of the pelvis), (2) Pelvic tilt (frontal plane rotation of the pelvis), (3) Knee flexion in the stance phase (knee sagittal rotation), (4) Foot mechanism (foot motion and dynamics during stance phase), (5) Knee mechanisms (knee motion and dynamics during stance phase), and (6) Lateral displacement of the pelvis (produced by relative adduction at the hip) (Saunders, 1953). These six determinants integrate together to minimize energy consumption, maintaining

a sinusoidal pathway of low amplitude for the center of gravity of the body. Based on the foot and knee mechanisms determinants, the motion of ankle, foot, and knee are closely related. For instance, during normal gait cycle, knee flexion after mid-stance is partly contributed by rapid plantar flexion of the foot, hence, there is enough clearance for the leg to swing without stumbling during the swing phase. It has also been extensively pointed out that when walking on level ground, the knee joint muscles absorb energy while many of the hip and ankle muscles are generating energy (Chen, 1997; Olney, 1994; Winter, 1983). Therefore, even with a prosthetic knee, which is able to produce exact function of the knee, without a proper cooperation and design of the prosthetic foot/ankle joint, it is unlikely to design prosthetic devices, which allow the transfemoral amputees to maintain the center of gravity at a similar sinusoidal pathway and minimize energy cost during gait cycle.

In spite of the fact that several prosthetic knees have been commercialized, and used for many years, none of them can mimic able-bodied ambulation, especially during the activities requiring more positive energy, such as stair climbing and running. Emerging designs are trending to elaborate the efficient energy flow at the knee joint by storing and releasing energy in a controlled way in a spring unit to obtain assisted gait. Yet, they have been tested under a limited array of conditions and their energy flow performance during the activities, other than walking at different pace, is still unknown.

The literature is missing a comprehensive analysis of energy flow at the knee and ankle joints during the activities of daily living. The analysis of impedance matching and the spring stiffness of the energy storage unit, which participates in harvesting and generating

the right amount of energy in a controlled way, is essential across the sub-phases of the gait cycle during a wide range of activities to understand the requirements of transfemoral amputee gait and design of energy regenerative devices. Next chapter investigates the healthy knee joint functional stiffness during the activities of daily living. The purpose of this work is to understand the importance of energy recovery, the moments, where energy needs to be harvested/returned and the importance of controlled energy flow at the knee joint in order to provide a fully/partial assisted gait in a more efficient and simpler way.

CHAPTER III

ACTIVE FUNCTIONAL STIFFNESS OF THE KNEE JOINT DURING THE ACTIVITIES OF DAILY LIVING

3.1 Introduction

Energy flow deficiencies due to a lack of positive work during the stance phase of gait for patients using controlled damping prostheses, led developers to consider emerging designs with controlled energy harvest/ return capabilities (Sup, 2008; Martinez-Villalpando, 2009; van den Bogert et al., 2012). The use of a spring in a prosthetic knee device theoretically reduces power demands and also provides high power-to-weight ratio (Argunsah and Davis, 2011). Therefore, instead of using heavy motors, gearboxes and bulky batteries, a spring can help the peak power demand of the prosthesis during the stance phase of gait with less weight. Moreover, adverse consequences such as circumduction and a disturbed gait pattern that take place due to the absence of positive energy delivery during the swing phase could potentially be alleviated by a energy-harvesting and timed-release system. Current generation powered designs deliver the needed energy with heavy battery demanding motors, which increase the mass of the device significantly, whereas, it needs to be relatively less than the mass of the missing portion of the

natural leg. Patients want lightweight prosthetics, capable of delivering natural gait by providing normal knee and ankle flexion angles during the activities of daily living (Aeyels, 1992).

Constant spring stiffness is suboptimal to varying gait requirements for different types of motion, due to the variability of the impedance (Pfeifer, 2011), functional stiffness and the power requirement of the knee caused by the passive characteristics, viscous and elastic attributes and the activation dependent properties of the muscles and their surroundings in the joint (Johns, 1962; Winters, 1988). These properties are altered instantaneously as the muscles are activated depending on the biomechanical demands of the performed activity and are closely linked to the instant stiffness of the joint. This adaptation is achieved through the active elasticity adjustment of the muscles in the joint. Thus, attaining this adaptation with controlled damper mechanisms, which are not capable of mimicking the activation dependent properties of the muscles and their surroundings in the joint, is hardly possible.

Passive stiffness, which is the measure of the flexion torque and the angle of the knee joint, during controlled perturbations without activating the muscles, has been investigated before (Yoon, 1982; Silder, 2006; Whittington, 2008; Mansour, 1986; Zhang, 1997). Pfeifer (2011) developed an active knee-stiffness analysis model, however, only level ground walking has been investigated in this study. Hansen (2004) has examined the ankle joint active functional stiffness during walking at variable cadence for guiding the prosthetic device designers in developing transtibial prostheses, which can optimize the energy flow at the ankle joint, yet, the authors are not aware of any prior work on the quantitative active knee joint functional stiffness analysis across a wide range of daily activities. In this study, dominant side knee joints of 12 subjects were examined for optimizing the knee joint functional stiffness with the aim of obtaining the best

possible quantitative values during the peak energy harvest and energy return phases of the activities of daily living (Table i).

3.2 Methods

3.2.1 Subjects

Twelve healthy, relatively young female and male volunteer subjects, (mean age: 30.42, SD: 4.87 yr.; mean height: 1.71, SD: 0.049 m; mean mass: 70.8, SD: 15.9 kg, mean BMI: 23.9, SD: 2.99 kg/m²) who do not have neuropathy and did not show any obvious gait abnormalities, participated in this study. All subjects were right-side dominant. Only people, whose body mass indices are within the 18.5-30 range were recruited for this study. Prior to testing, each subject read and signed an informed consent that was approved by the Cleveland Clinic Foundation Institutional Review Board.

Measure	Activity						
	Stair Ascent	Stair Descent	Sit/Stand/Sit Sequence	Slow Walking	Normal Walking	Fast Walking	Slow Running
Cadence (steps/min)	75.2±4.5	86.3±7.5	35.5±4.2	101.9±7.3	113.9±7.6	125.3±11.8	157.9±10.1
Step Length (cm)	26.8±7.3	32.2±7.8	0.012±1.37	63.4±8.5	72.1±8.4	78.2±9.8	91.8±12.3
Step Width (cm)	10.6±4.5	12.09±4.7	28.1±7.3	12.0±2.6	12.5±2.5	11.9±2.5	11.6±2.9
Forward Vel. (cm/s)	40.4±4.1	44.1±8.3	0.65±0.4	108.4±16.3	138.4±18.4	166.6±24.7	242.7±33.2

Table i: Means (\pm SD) of spatio-temporal measures for the dominant side across the activities (n = 12)

3.2.2 Experimental Protocol

The motion analysis system used in the Cleveland Clinic's "Doris Alburn Musculoskeletal Performance Laboratory" consisted of an eight-camera motion capture systems (Motion Analysis Corporation, Santa Rosa, CA) and an AMTI force plate, embedded into the floor Serial No. 4046 (AMTI Force and Motion, Watertown, MA). Each subject was set up with 34 Motion Analysis Corporation retroreflective markers using the Cleveland Clinic marker set which attaches the markers to represent joints and specific bony landmarks. Twelve of the markers were composed of triangle marker sets (19 mm) and placed on the right and left thigh and shank of the subject. The remaining marker placements include the right and left shoulder, right and left elbow, right and left wrist, lateral and medial knee and ankle, left and right anterior superior iliac spine, sacrum, right and left heel and toe and an offset placed between the right shoulder and elbow. All subjects walked with soft-soled gym shoes. Prior to data collection two standing collections were taken to confirm the visibility of all the markers with the system. Three good walking collections were taken prior to data collection in order to obtain a consistent locomotion rhythm during walking at variable cadence and slow running activities.

3.2.3 Data Analysis

A standard patient testing protocol was developed and the same routine was followed for each subject. The testing program included slow/normal/fast walking, slow running, stepping up 18 cm riser-31 cm deep steps, down the same steps, sitting on an armless chair, and rising from an armless chair. Five acceptable trials of the right foot squarely striking the force plate were collected and averaged (mean \pm SD) to represent each collected parameter. An acceptable trial

was obtained as long as the subject appropriately stepped on the force plate with the intended foot while maintaining the desired ambulation rhythm for walking and running trials. For stair ascent/ descent and sit/ stand/sit sequence trials, full contact with the force plate with the intended foot was defined as an acceptable trial.

Data Analysis was done by Cortex (marker and motion tracking), OrthoTrak (kinetic and kinematic analysis of the knee joint for each parameter), Microsoft Excel and Matlab (Mathworks, Natick, MA, <http://www.mathworks.com>) (data reduction). Images were collected at 60 Hz by the Motion Analysis and at 1200 Hz in sync with AMTI force plate. Knee joint kinetic and spatial/temporal kinematic parameters were collected for both legs. The foot contact and ground reaction forces were used to determine the percentages of stride, which were normalized to 100%, for each activity. Lengths of lower limb segments, using the landmark locations as references, were manually measured, along with subject height, weight, foot length and dominant side information.

Knee joint powers were calculated for each trial by rotating the joint velocity into the distal segment's coordinate system and then multiplying by the segment's sagittal plane moment. The peak energy harvest and return intervals were identified from the power vs. percentage of stride curves for each activity, then the functional stiffness rates during the peak energy return (R_{max}), and peak energy harvest (H_{max}) phases were presented and optimized for the tested activities.

Knee joint functional stiffness was calculated by fitting a linear line to the sagittal plane knee flexion moment versus knee flexion angle curves for peak energy harvest and return phases. The slopes of the torque versus knee flexion angle curves were defined as the functional-stiffness required during these intervals.

The purpose of the functional stiffness optimization was to find the most advantageous quantitative functional stiffness value required for the prosthetic knee in order to obtain the best possible ambulation during the tested activities of daily living with a single energy-storage unit.

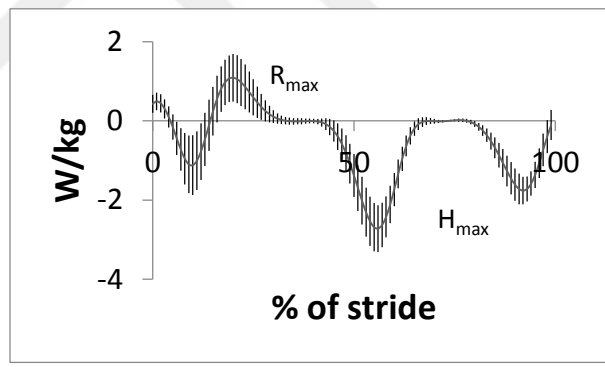
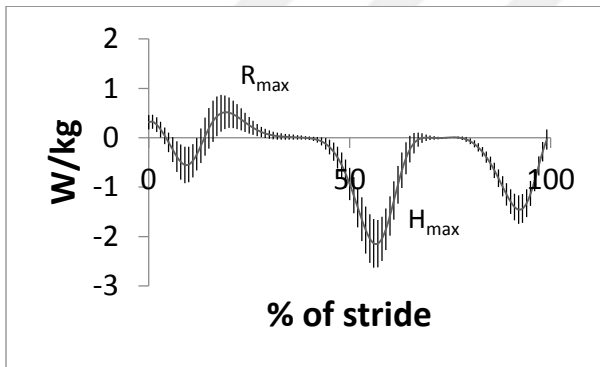
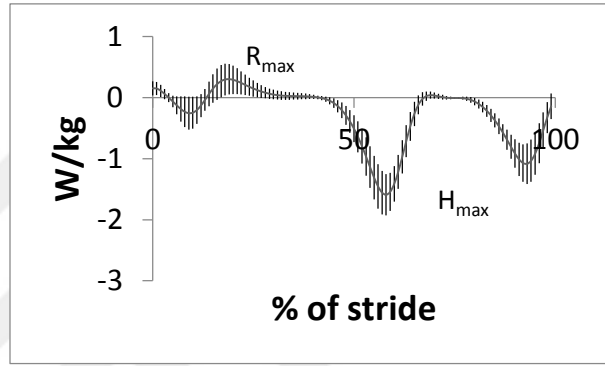
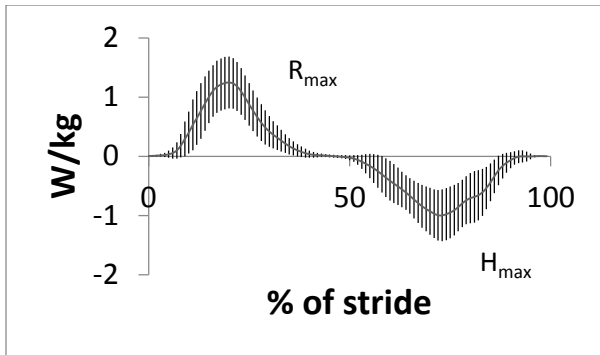
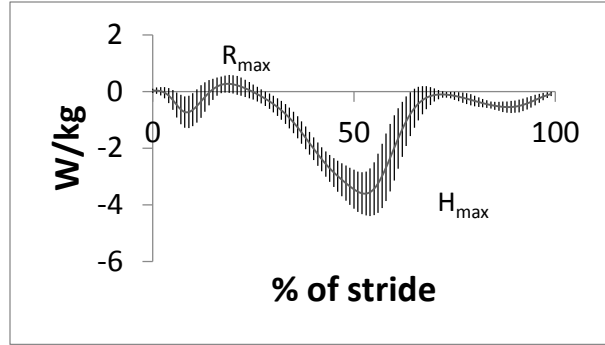
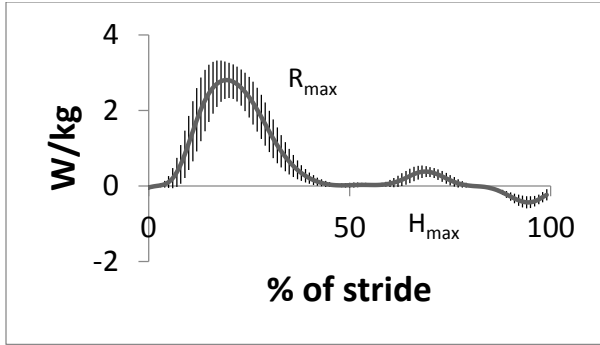
3.3 Results

3.3.1 Knee Power Profiles

The overall energy flow patterns for 12 subjects were calculated and presented for the dominant side knee joint during the activities of daily living. The peak energy harvest and return phases were determined and the quantification of the functional stiffness was done according to these profiles. The positive power peaks, where energy is dissipated, indicated the intervals where the spring releases the stored energy, contrarily the negative power peaks, where energy is harvested in the system, indicated the intervals where the spring compression and energy storage occur. The identification of the peak energy return and harvest phases was done according to the magnitude of the total area under the power vs. percentage of stride curves (Figure 2). The maximum positive work peak was identified as the R_{\max} and the maximum negative work peak was identified as the H_{\max} for each activity (Table 2). The areas under the R_{\max} and H_{\max} curves are calculated by;

$$R_{\max} = \max W_i^{\text{positive}} \text{ Where } W_i^{\text{positive}} = \int_{t_i}^{t_f} P_{d_i} \quad (1)$$

$$H_{\max} = \max W_i^{\text{negative}} \text{ Where } W_i^{\text{negative}} = \int_{t_i}^{t_f} P_{d_i} \quad (2)$$



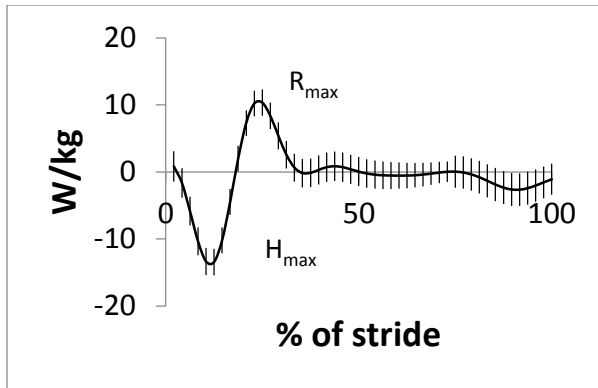


Figure 2: Averaged power profiles (mean (SD)) at the knee joint across the activities of daily living: Stair ascent, stair descent, sit /stand/ sit sequence, slow/ normal/ fast walk and slow run respectively with the peak energy return (R_{max}) and harvest (H_{max}) phases

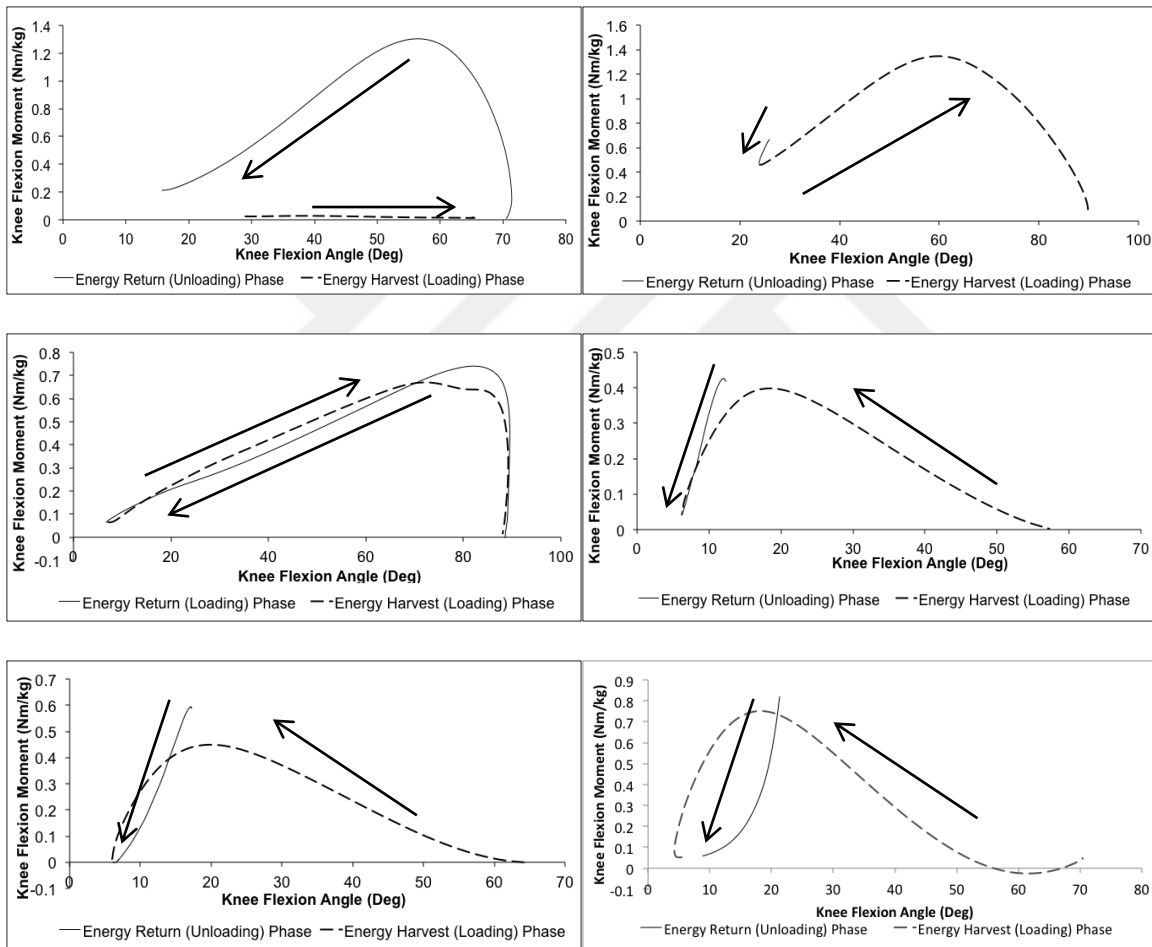
GAIT ACTIVITY	Max. Energy	Energy	Max. Energy	Energy
	Return	(J/kg)	Harvest	(J/kg)
Stair ascent	R_1	0.840 ± 0.127	H_1	0.064 ± 0.021
Stair descent	R_1	0.040 ± 0.038	H_2	1.115 ± 0.191
Sit/stand/sit	R_1	0.364 ± 0.105	H_1	0.346 ± 0.117
Slow walking	R_2	0.043 ± 0.035	H_2	0.212 ± 0.043
Normal walking	R_2	0.058 ± 0.041	H_2	0.261 ± 0.047
Fast walking	R_2	0.096 ± 0.057	H_2	0.294 ± 0.057
Slow running	R_1	0.491 ± 0.159	H_1	0.581 ± 0.190

Table ii: Averaged energy flow during the activities of daily living, indicating the required energy during the unloading phases and the harvestable energy during the loading phases

3.3.2 Functional Stiffness Analysis

The peak energy return and energy harvest trajectories of the knee torque vs. knee flexion angle curves were presented in order to obtain the functional stiffness for each activity (Table 3).

The slopes of the moment-angle properties during energy harvest and return phases were specified as the functional stiffness for the analyzed daily activity (Figure 3).



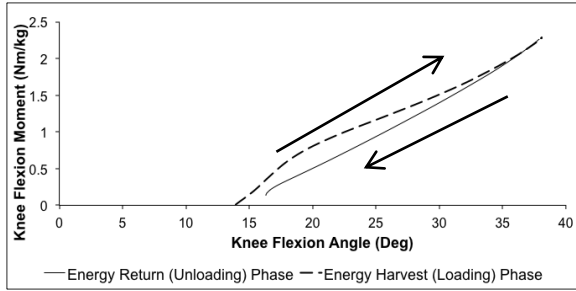


Figure 3: Knee joint peak energy return and harvest phase functional stiffness profiles during stair ascent, stair descent, sit/stand/sit sequence and slow/normal/fast walking and slow run respectively. The upward direction of the arrows indicates the spring compression to harvest energy; contrarily downward direction of the arrows indicates the spring release to return energy back to the system.

GAIT ACTIVITY	Max. Energy Return Phase	Return phase Stiffness (Nm/kg deg.)	Max. Energy Harvest Phase	Harvest phase Stiffness (Nm/kg deg.)
Stair Ascent	R ₁	0.013	H ₁	0.000
Stair Descent	R ₁	0.023	H ₂	0.012
Sit /Stand/ Sit	R ₁	0.006	H ₁	0.006
Slow Walking	R ₂	0.025	H ₂	0.005
Normal Walking	R ₂	0.026	H ₂	0.004
Fast Walking	R ₂	0.031	H ₂	0.003
Slow Running	R ₁	0.046	H ₁	0.052
AVERAGE	R	0.024 (SD:0.013)	H	0.011(SD: 0.018)

Table iii: Functional stiffness during the activities of daily living

During stair ascent activity, zero stiffness was obtained during energy harvest phase, which indicated that a spring unit would not be able to store energy by being compressed due to the infinite rigidity of the knee joint. Therefore augmented mechanisms, such as motors, were

required to produce the required positive energy when needed during this activity. For the rest of the tested activities, a controllable passive, yet spring-damper comprising system would provide a smooth transition between the states of the performing activity and the required positive work can be produced/ returned back to the system when required in a controlled way. During sit/stand/sit sequence, same functional stiffness values were obtained for energy return and harvest phases, which indicated that this activity is a cyclic activity and the stored energy is sufficient to provide the required energy when it is needed. Therefore, a single spring would be satisfactory in obtaining adequate movement for this activity. However, for stair descent and walking at variable cadence activities, no net positive work is needed at the knee joint, which implies that a motor use in a prosthetic knee design for these activities would be unnecessary as well.

3.4 Discussion

Functional stiffness defines the elastic resistance when movement takes place at the muscle. It is the measure of the rigidity of the joint and it varies depending on the state of the stride as well as the performed activity. This work investigated the functional stiffness of the knee joint during the activities of daily living and presented the average rates for the peak energy return (0.024 (SD:0.013)) and harvest phases (0.011(SD: 0.018)).

Low functional stiffness rate indicates that the muscle is relatively rigid and it does not flex easily, on the other hand high functional stiffness value indicates that the muscle is less rigid and can flex easily. Zero functional stiffness means that the muscle is extremely stiff or rigid, that it does not bend at all. During the energy harvest phase, the resistance to motion was decreased;

and energy is generated at the muscle. Therefore, low stiffness value, which is the indication of low elastic resistance at the knee joint, was obtained during the loading phases of each activity. Consequently, the increased joint displacement allowed muscle contraction in the opposite direction of the rotation and energy storage. Moreover, during the energy return phases, due to the knee joint's assistance to the imposed deformation caused by a reversal of the usual directional relationship between the applied torque and angle, higher functional stiffness values were obtained, which indicated energy dissipation at the muscle. Therefore, only a small displacement occurred at the knee joint and more closely aligned ground reaction vector with the ankle, knee, and hip joints, was obtained which urged the knee joint to resist rotation and burn the stored energy.

The variability in functional stiffness values during the energy return and energy harvest phases as well as across the daily activities indicated the difficulty of achieving high efficiency by a simple mechanism. A prosthetic knee, which is capable of mimicking the healthy knee by harvesting and returning energy in a controlled way, requires the support of smart systems such as microprocessors, valves, pumps, motors etc. to supplement their pure mechanical components through adjusting the amount and timing of the spring compression/ release instantaneously depending on the biomechanical demands of the performed activity. Since it is not realistic to use different springs for different activities, the most effective solution would be obtaining variable stiffness with some hardware modifications, such as parallel oriented spring couplings and series of elastic actuators.

Walking at variable cadence, slow running and sit/stand/sit sequence are cyclic activities, which do not require a motor in order to provide the needed positive work to the knee joint

(Winter, 1983; Sup, 2008; Martinez-Villalpando, 2009). During the activities, which are not cyclic and also either require net positive energy or do not have sequential positive and negative energy intervals throughout the gait cycle, a simple spring mechanism would be insufficient in achieving fully assisted and energy regenerative gait. Therefore, it is anticipated that, without a motor use or some hardware modifications, such as parallel oriented spring couplings and series of elastic actuators, transfemoral amputees would be performing activities, which are not cyclic and also either with a step-by-step technique where the healthy leg leads while the prosthetic limb follows it passively, or with asymmetrical posture and abnormal movement of the amputated side hip joint.

In designing transfemoral prostheses, which harvests energy from the movement of the user and instead of releasing the harvested energy immediately, keeps it until the energy is most needed during the swing phase is crucial for achieving assisted and energy regenerative ambulation. During stair ascent activity, the use of a motor would be necessary in order to produce the required net positive work, which cannot be delivered by the spring compression, as the functional stiffness during this activity was zero, which indicated that the torque-angle properties of the knee joint during stair ascent did not allow spring compression thru knee flexion. With the exception of the stair ascent activity, a spring and accompanying mechanical and electrically controlled mechanisms would be an effective way to control the amount and timing of the spring compression and release with the purpose of obtaining the required knee joint stiffness. Next study investigates the development of a prosthetic knee test protocol with the aim of analyzing the prosthetic device functional stiffness and the obtained gait symmetry.

CHAPTER IV

MECHANICAL SIMULATION OF HIP JOINT DURING WALKING FOR EVALUATION OF PROSTHETIC KNEE FUNCTIONAL STIFFNESS

4.1 Introduction

Transfemoral amputation is one of the most traumatic medical treatments an amputee can receive. Along with the decrease in the physical function and neural feedback, amputees also have a degraded gait after amputation. There is insufficient shock absorption during stance phase and disturbed pelvic movement during swing phase due to the fact that the prosthetic knee does not flex sufficiently and the patient therefore has to elevate their hip to allow the foot to clear the ground. These strategies result in abnormal gait patterns even with the most sophisticated microprocessed prosthetic knee available on the market today (Kulkarni, 2005; Gailey, 2008; Modan, 1998). Therefore, the emerging developments focus on the efficient energy flow at the knee joint (Sup et al, 2008; Martinez-Villalpando et al, 2009; van den Bogert et al., 2012). These new prosthetic devices require several testing techniques for performance evaluation, such as

dynamic *in vitro* testing, able-bodied human testing by using wearable adaptors, wear and robotic simulations. Although clinical testing provides the most realistic biomechanical conditions, there are several issues (use of a safety harness, lack of repeatability etc.), which make the data collection process difficult and sometimes impractical. Moreover, subjects' physiological and psychological conditions, physical characteristics, prosthetic device familiarity, gender and age are some of the factors which affect prosthetic device performance evaluation. Similarly, enough acclimation time should be given to the subject to ensure that he/she is able to ambulate with the tested prosthetic device comfortably so that the new prosthetic device performance is not affected by any personal influence. Consequently, providing consistent biomechanical conditions, eliminating the subject variability and being able to mimic the close to normal loading during every iteration, as well as the repeatability of the desired conditions several times make the wear and robotic simulation techniques preferable over human testing.

Wear simulators have been used previously with the purpose of testing prosthetic devices by applying repetitive loading cycles to the hydraulic or pneumatic element of the device (Walker et al, 1996; Currier et al, 1998). Whereas, realistic loading conditions cannot easily be obtained with this type of testing as both the femur and foot are connected to the simulator, maximum stress testing during loading and the durability testing are performed satisfactorily.

Musculoskeletal robotic simulation provides free tibia-foot movement as well as close to normal dynamic loading by simulating the motion and real time dynamics of physiological loading conditions of joints. Musculoskeletal simulators have been used

previously for testing the prosthetic knee devices by reproducing the forces, moments, and motions of hip, knee and ankle joints during the activities of daily living (Guess and Maletsky, 2005; Maletsky and Hillberry, 2005; Unal et al, 2010). The prosthetic knee is screwed to the simulator vertically and its femur end is connected to the posterior of the patella. When the connection between the distal posterior of the femur and proximal posterior of the tibia is obtained, simulator starts reproducing the hip joint movement and the physiological dynamics that would occur during the use of an above knee prosthesis.

The purpose of this study was to develop a prosthetic knee test method for evaluating the mechanical response of the prosthetic knee joint by iteratively modifying the hip trajectory until achieving the closest to natural walking biomechanics by using a 3 DOF simulator (Figure 7).

Obtaining the favorable ground loading with a passive prosthetic knee are crucial in achieving the normal loading and ideal propulsion. The dampening of the Mauch Microlite S Knee was evaluated in order to calculate the knee joint functional stiffness and its kinetic/ kinematic parameters were compared with a healthy knee joint. This work focuses on the mechanical behavior of the healthy knee and pure passive prosthetic knee by evaluating the behavior of the knee in the flexion and extension modes of the weight acceptance stage.

4.2 Materials and Methods

4.2.1 Materials

4.2.1.1 Mauch Microlite S Transfemoral Prosthetic Knee

Mauch Microlite S, a purely passive friction-based prosthetic knee allows amputees to walk at various speeds via using hydraulic fluid flow to control the piston as it forces fluid out of the staggered holes to simulate the muscle movement (US Patent 5092902). It does the reverse process for the extension stroke of the swing phase to simulate flexion and extension and provides variable plus adjustable damping forces during flexion and extension of the knee joint through manipulating the direction of the restricted hydraulic fluid flow.

A hydraulic unit is composed of a piston, oil reservoir and gas pressurized bladder. The oil reservoir comprises a group of gaps, which open/close as the piston moves axially depending on the instantaneous biomechanics of the performed activity and permit/prevent the hydraulic fluid flow. As the body weight is applied on the hydraulic cylinder, the piston moves in the downward direction and increases the pressure of the gas bladder to produce the needed damping forces.

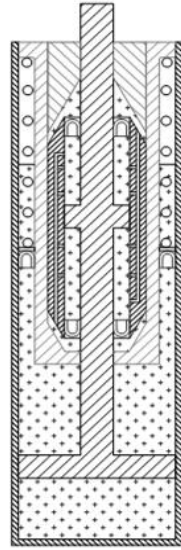


Figure 4: Mauch SNS Knee hydraulic cylinder

The hydraulic unit contains two annular valves (Figure 4). The upper annular valve, which is made of titanium, is activated during the swing phase and initiates the hydraulic fluid flow in the upward direction and decreases the pressure in the gas bladder, which permits smooth knee joint flexion. The lower annular valve, which is made of brass, is activated during the stance phase and initiates the hydraulic fluid flow in the downward direction and increases the pressure in the gas bladder to provide the needed loading. As the oil temperature increases after continuous use of the prosthetic knee, the brass valve narrows down and compensates the reduced viscosity of the hydraulic oil.

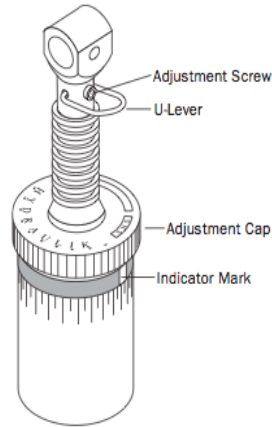


Figure 5: The Rotating Dial on the Hydraulic Unit (Instructions for Use, www.Össur.com)

The rotating dial (Figure 5) permits the user to select the degree of stiffness of the damping program, which allows ambulation at a variable cadence. The valve, which is sensitive to the direction of flow in the cylinder, adjusts the knee stiffness during swing and stance phases.

During the stance phase, hydraulic fluid flows through the narrow orifices in the valve, which increases the stiffness and provides the needed weight bearing support. During the swing phase, as the valve opens, hydraulic fluid flows through the wide orifices and permits the knee joint flexion.

4.2.1.2 Össur Flex-Foot Assure

Flex Foot Assure (Figure 6) is a purely passive, yet energy responsive prosthetic foot, which was designed for the less active starter prosthetic users. It incorporates an active heel and a full-length keel, to achieve the needed weight bearing depending on the

applied force and provide smooth and flexible movement by means of its active transtibial progression feature (<http://www.Össur.com>, Flex-Foot Feet).

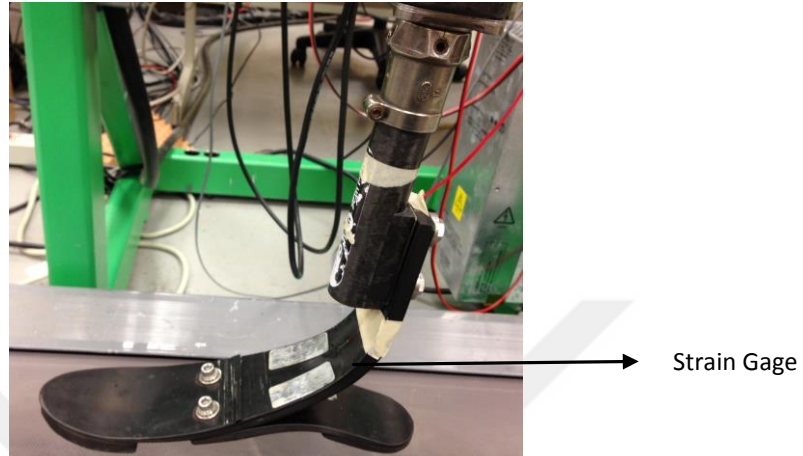


Figure 6: Ossur Flex Foot

4.2.1.3 Prosthetic Knee Simulator

3 DOF Simulator system was built at Cleveland State University and used to replicate the hip vertical displacement and hip swing (rotation in sagittal plane) of a healthy human during normal walking (105.88 steps/min). During the swing phase feedback was motion-based only and the simulator tracked the hip rotation and hip vertical displacement of the input reference profile. During the stance phase, the simulator continued to track the reference hip rotation and at the same time the hip vertical displacement was adjusted in order to achieve the desired ground contact forces. In this phase, feedback was motion and force based.

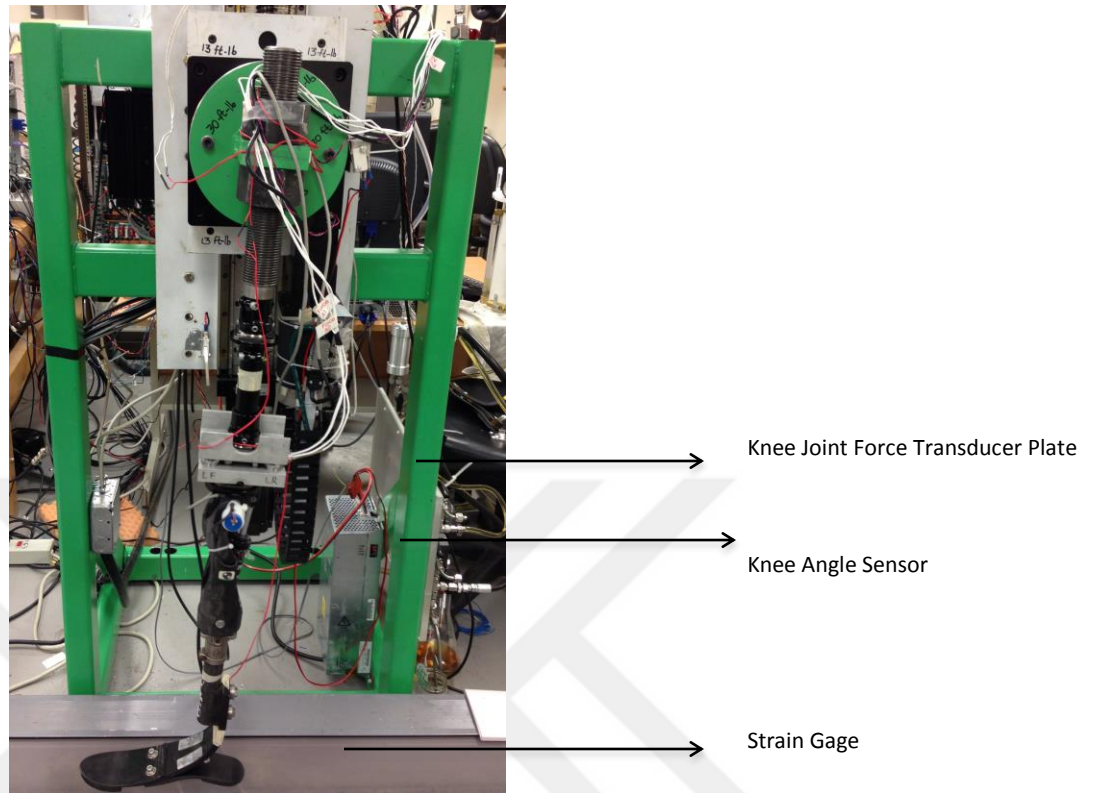


Figure 7: Complete Simulator Assembly: A speed-adjustable treadmill was used as the ground surface during testing. A Mauch Microlite S knee was attached to the rotary plate by an adjustable threaded rod, which is secured to the plate with two 2.75- inch nuts. The lengths of the femur and tibia were measured as 16.5 inch.

4.2.2 Methods

2-DOF movement at the hip joint was reproduced whilst the ground loading was controlled by the vertical load motor, which applied downward forces to create femoral loading (Figure 8). The hip vertical displacement and rotation profiles were modified iteratively until the gait which delivered the approximated to normal GRF profile during normal walking was achieved. Since the moment of inertia due to the mass of the rotary and vertical motor assembly and the mounting rod (~14 kg) are significantly higher than

the mass of the prosthetic knee assembly (1380 g), the moment of inertia due to the weight of the tested hardware was neglected. Manual hip vertical displacement bias control was used to descend the Flex-Foot to the treadmill while the strain gage reading was monitored continuously. The speed of the treadmill was manually synchronized to the foot velocity during contact in order to prevent slippage.

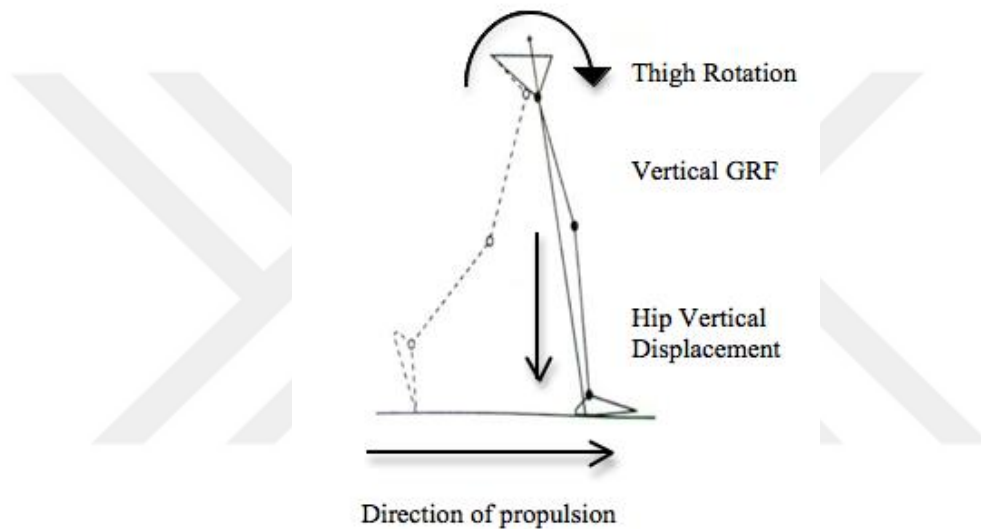


Figure 8: Illustration of the GRF iteration variables

Matlab (Mathworks, Natick, MA, <http://www.mathworks.com>) and LabView (National Instruments Corporation, Austin, TX, <http://www.ni.com>) were used for data collection. The outputs of the simulation were the ground reaction force, knee flexion angle and knee flexion moment during normal walking.

4.2.2.1 Iteration Rules

Desired ground loading was achieved by selectively modifying three variables. Single iteration rule was changed during each iteration by following the sequence described below:

1. Hip vertical displacement trajectory: was changed until the desired loading was obtained at the knee joint while the normal walking biomechanics of an 85 kg healthy human was simulated.

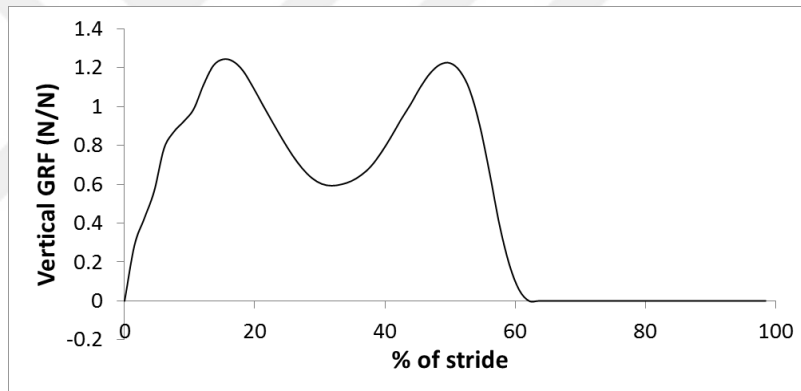


Figure 9: Healthy Human Normal Walking Vertical GRF Profile (Source: Cleveland Clinic, Lerner Research Institute, Biomedical Engineering Department- Cleveland, OH. “Energy Flow Studies Human Gait”)

1.2 N/N ground loading is achieved during the first single limb support period (~15% of gait cycle) when weight acceptance occurs at the knee joint. As the complete body weight is carried by the grounded foot, the weight acceptance reaches its maximum value during this resistive flexion stage. Then the knee extends again until it hits a maximum extension and starts to flex which results in a decrease in applied loading

(~30% of stride). At 50% of gait (second single limb support), propulsive extension is observed and this period ends with toe off. The ground loading reaches its lowest level during the beginning portion of this period as both feet are in contact with the ground. Then the ground loading starts to increase until the opposite foot heel strike at the end of the stance phase is observed and reaches the maximum ground loading for the second time. Subsequently, as the swing phase is initiated (last 40% of stride) the body weight is transferred to the opposite limb and the GRF reaches the minimum value. The vertical displacement profile was modified until the best matching loading was achieved, in terms of the number of the vertical GRF peaks as well as the magnitude and duration of the peaks during the first single limb support (Figure 9).

2. Hip angle trajectory: the hip extends throughout the first single limb support as the limb progresses from an anterior to a posterior position to transfer the body weight from one limb to another. The knee extends again until it hits a maximum extension and starts to flex. During the propulsive extension period of the weight acceptance stage, the hip extends and prepares for the limb's lift off. The hip angle trajectory was reproduced until the second GRF peak was obtained during the 50% of gait cycle.

3. Deceleration before heel strike: after obtaining the desired ground loading profile with two peaks, in order to achieve the ideal loading time and propulsion, the swing bias of the simulator was reproduced until the desired ground loading timing was obtained.

4.3 Results

4.3.1 Ground Loading Iteration Results

The following charts show the attempts to obtain the closest to normal ground reaction loading and propulsion profile with the pure passive Mauch Microlite S prosthetic knee. Therefore, by following the same iteration sequence, any prosthetic knee+ prosthetic foot system could be tested and evaluated in terms of symmetry of gait and naturalness of propulsion.

4.3.1.1 Hip Vertical Displacement Iterations

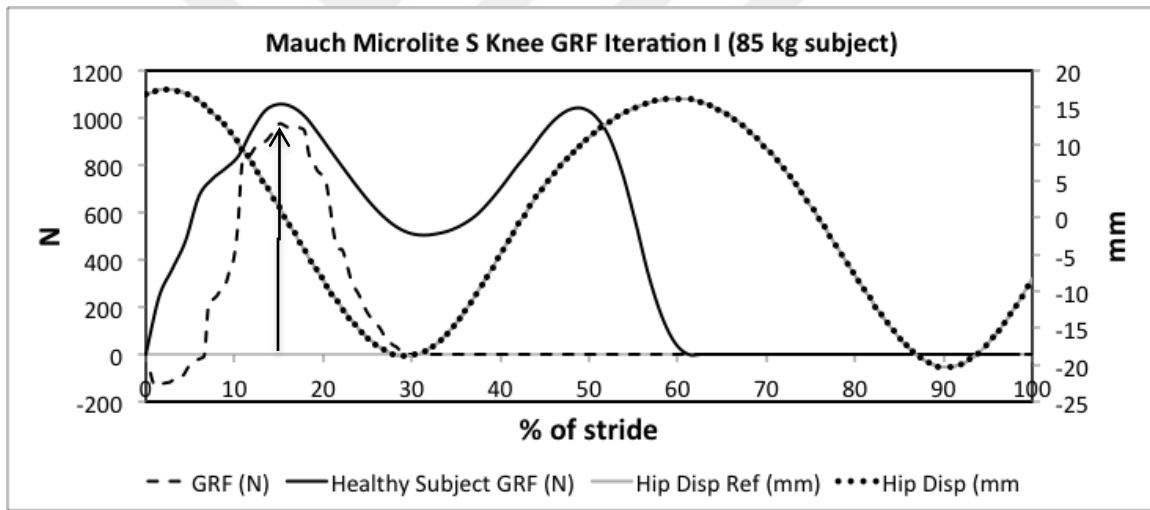


Figure 10: Mauch Microlite S Knee GRF Iteration I: Original height of the linear slide: 1016 mm, Iteration I- Height of the linear slide: 1016 mm

The timing of the first GRF peak was achieved with the original hip displacement trajectory (15% of stride). However, the desired magnitude of the loading (1000.3 N) could not be obtained. Moreover, the ground loading was up to 30% of stride, which indicated the abnormal and significantly short stance phase due to the insufficient loading (Figure 10).

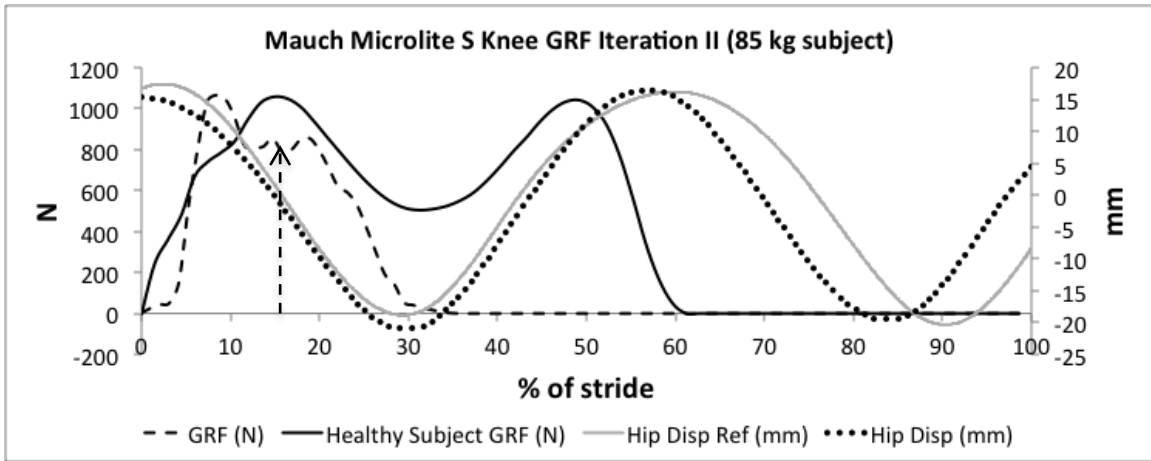


Figure 11: Mauch Microlite S Knee GRF Iteration II: Original height of the linear slide: 1016 mm, Iteration II- Height of the linear slide: 1016-53.6 mm

The desired timing, duration and the magnitude of the resistive flexion stage peak were obtained, however, the foot landed on the treadmill earlier than the desired time since, the GRF curve reached the highest value at the 8% of stride. Although the loading time slightly increased (from 30% to 35% of stride), symmetrical gait was not obtained due to the insufficient and significantly short loading (Figure 11).

4.3.1.2 Hip Angle Iteration

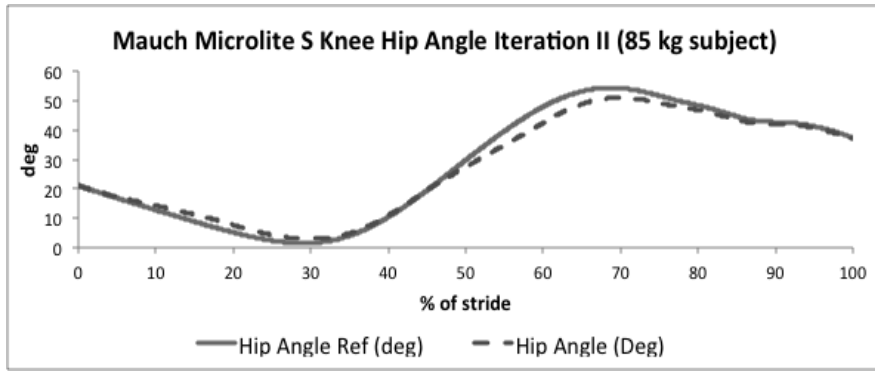


Figure 12: Hip angle trajectory iteration

The hip angle trajectory was modified until the desired timing and the magnitude of resistive flexion and propulsive extension stage peaks were obtained along with a longer ground loading period (Figure 12).

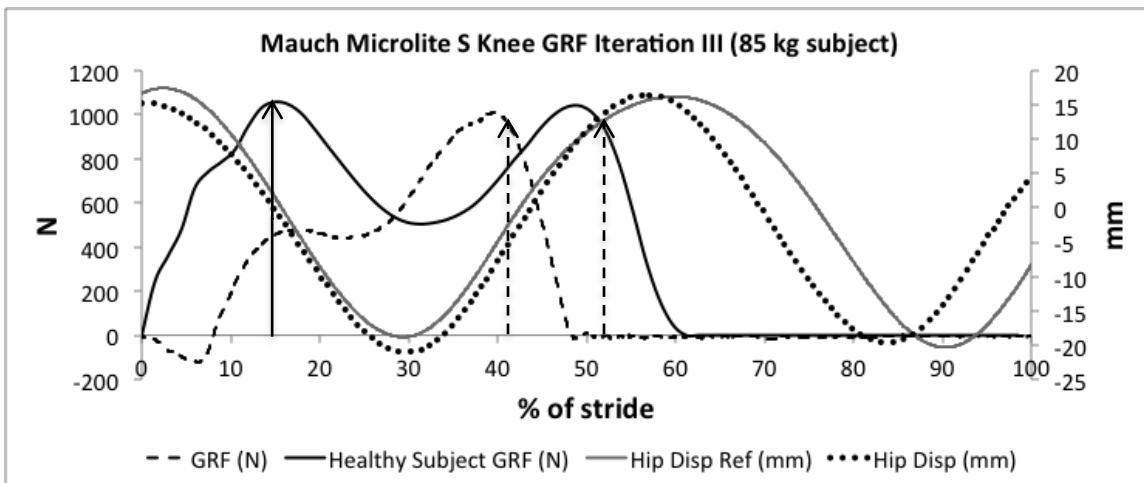


Figure 13: Mauch Microlite S Knee GRF Iteration III: Original height of the linear slide: 1016 mm, Iteration III- Height of the linear slide: 1016-71.7 mm

Desired timing was achieved only for the resistive flexion stage peak, however the magnitude of the loading did not match. Desired ground loading was achieved for the propulsive extension stage peak, however the desired timing was not obtained. Additionally the ground loading was up to ~48% of stride only (Figure 13).

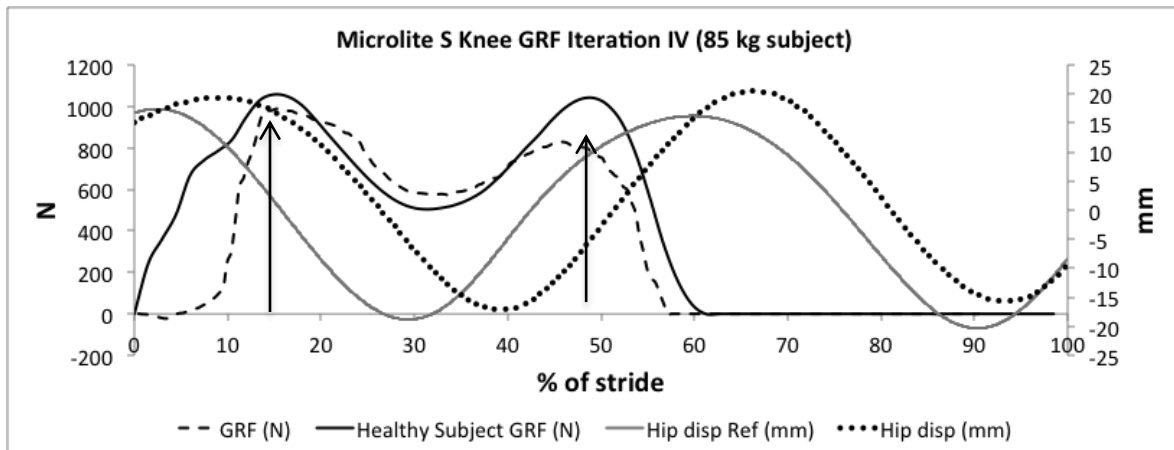


Figure 14: Mauch Microlite S Knee GRF Iteration IV: Original height of the linear slide: 1016 mm, Iteration IV- Height of the linear slide: 1016-86.5 mm

Desired timing and magnitude were achieved both for the resistive flexion and propulsive extension stage peaks with ground loading up to ~58% of stride (Figure 14).

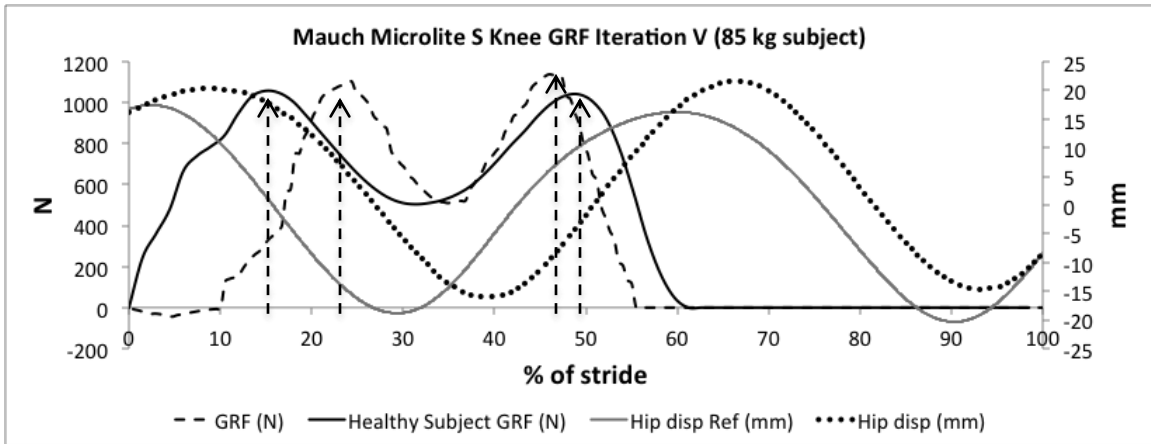


Figure 15: Mauch Microlite S Knee GRF Iteration V: Original height of the linear slide: 1016 mm, Iteration V- Height of the linear slide: 1016-93.3 mm

Desired magnitude was achieved both for the resistive flexion and propulsive extension stage peaks, however the timing of both peaks did not match. The ground loading was up to ~55% of stride (Figure 15).

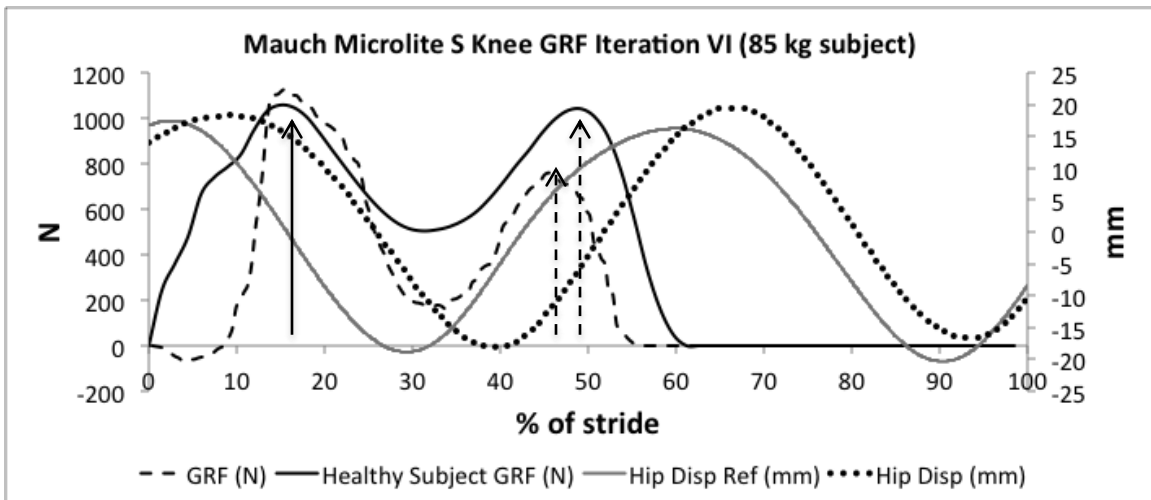


Figure 16: Mauch Microlite S Knee GRF Iteration VI: Original height of the linear slide: 1016 mm, Iteration VI- Height of the linear slide: 1016-96.3 mm

Desired magnitude and timing were achieved during the resistive flexion stage peak. However, neither timing nor magnitude was obtained during the propulsive extension stage peak. The ground loading was up to ~55% of stride (Figure 16).

Iteration IV was chosen as the closest to normal ground loading profile, which would provide the desired GRF and propulsion due to the:

- Matching resistive flexion and propulsive extension stage peak timing
- Matching GRF during the resistive flexion and propulsive extension stage peaks
- Closest to healthy subject stance phase loading time (~60% of stride)
- Minimum negative force reading during the initial loading phase (2-5% of stride)

4.3.2 Robotic Analysis of the Mauch Microlite S Knee Joint Functional Stiffness

Functional stiffness defines the elastic resistance when movement takes place at the joint. It is the measure of the rigidity of the joint and it varies depending on the state of the stride as well as the performed activity. In terms of energy storage in prosthetic knee devices, functional stiffness is the degree of achieved weight bearing during the resistive flexion stage of stance phase (0-15 % of stride). This is the only moment when energy can be stored at the prosthetic knee, due to the high knee flexion moment and low knee flexion angle behavior of this interval. The prosthetic device should provide the needed flexion during this phase in order to achieve energy regenerative gait by storing the available energy by applying a large moment and returning it back to the system when positive energy is required during push off for a smooth and natural ambulation during the rest of the stride while supporting the body weight.

In order to evaluate the gait symmetry, normal walking biomechanics during the resistive flexion stage peaks of the healthy knee joint (Figures 9, 17) and Mauch Microlite S knee (Figure 19) were analyzed. Clinical analysis of the knee joint flexion moment and flexion angle profiles was compared to the robotic simulation of the pure passive prosthetic knee flexion moment and flexion angle profiles (Figures 18, 20).

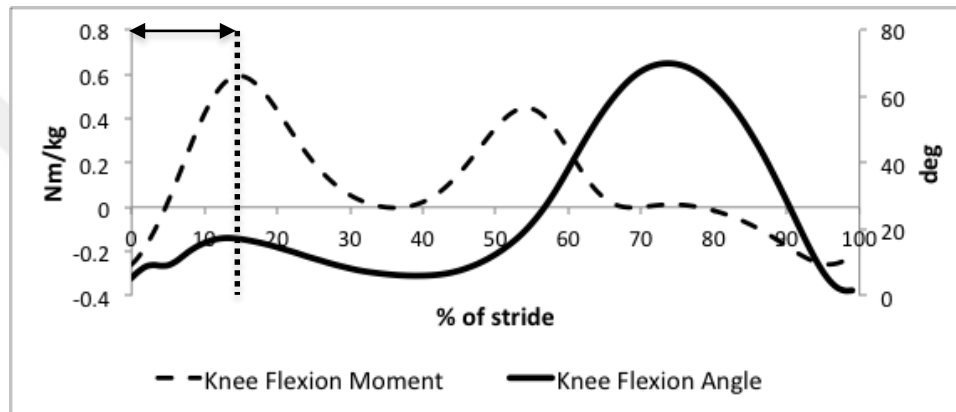


Figure 17: Healthy Knee Joint Normal Walking Biomechanics

Knee joint functional stiffness was calculated by fitting a linear line to the sagittal plane knee flexion moment versus knee flexion angle curves during the first 15% of the gait cycle (Figure 19).

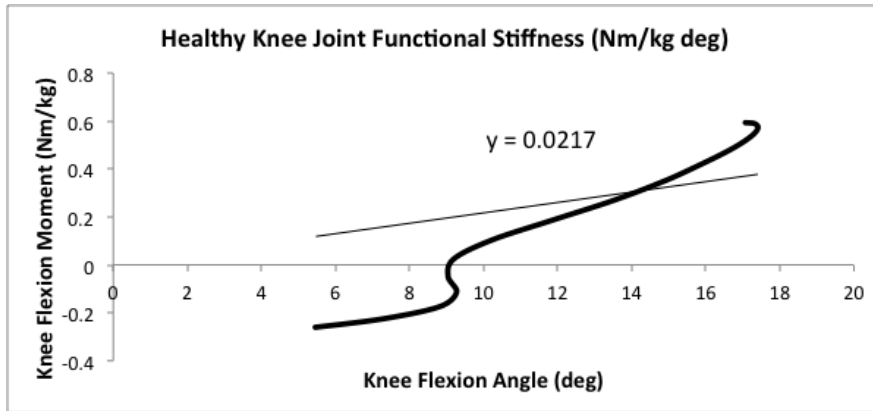


Figure 18: Healthy Knee Joint Normal Walking Functional Stiffness during the resistive flexion stage of gait

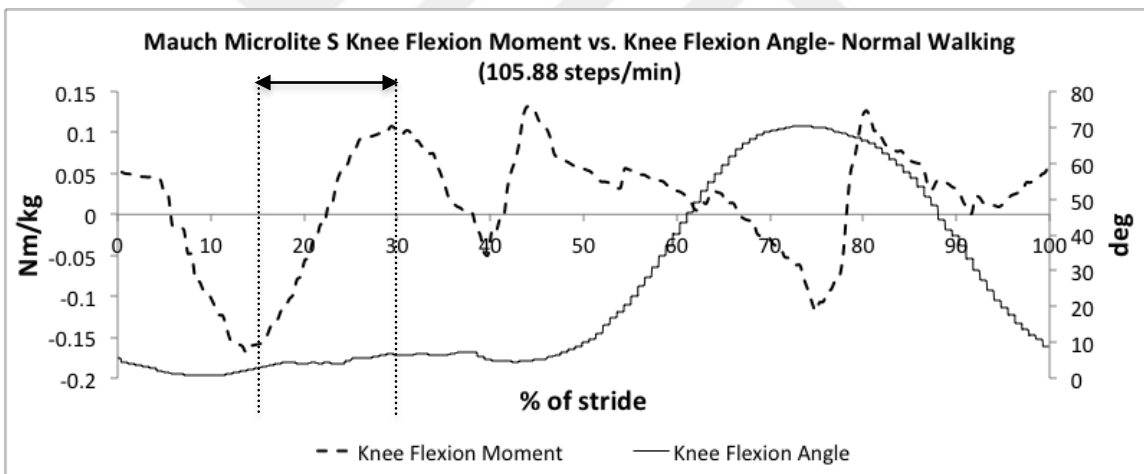


Figure 19: Mauch Microlite S Knee Normal Walking Functional Stiffness during the resistive flexion stage of gait: Iteration IV Knee joint Torque-Angle properties during first ~15-30% of stride, where resistance to motion was decreased to store the available energy

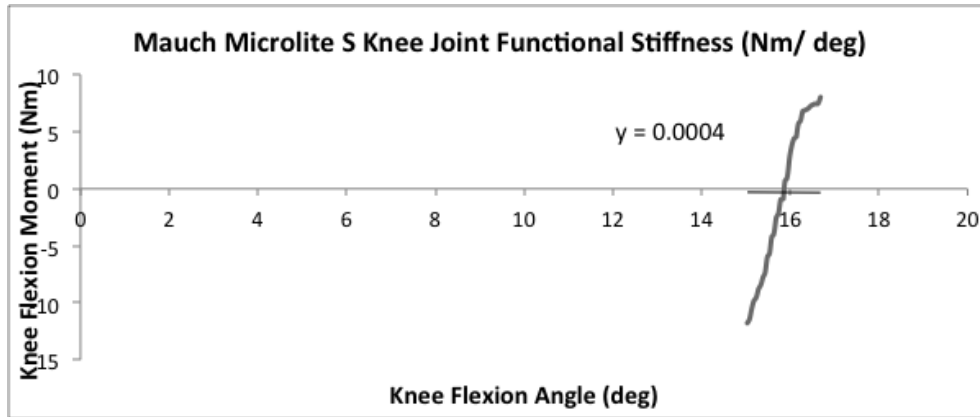


Figure 20: Mauch Microlite S Knee Functional Stiffness for the resistive flexion stage of the “optimum” ground loading condition (Iteration IV) during normal walking, the most energy efficient activity of daily living

4.4 Discussion

Knee joint functional stiffness was evaluated both clinically and robotically. Healthy knee joint torque- angle properties were compared to the pure passive Mauch Microlite S knee torque-angle properties during the “closest to normal” ground loading condition. Healthy knee joint functional stiffness during the resistive flexion stage was 0.0217 Nm/kg deg; same value for the Mauch knee was 0.0004 Nm/kg deg, which indicated that the Mauch knee was relatively rigid and did not mimic the normal walking due to the insufficient/ missing knee flexion during the energy harvestable phase, where the prosthetic knee is expected to flex and store the available energy. Since the knee was rigidly locked in the stance phase, natural gait was not demonstrated. Contrarily, during the late stance and swing phases, knee flexion angle profiles were significantly close to the healthy knee joint knee flexion angle curve (Figure 21).

The existing arrangement allowed the implementation of human-like leg compliance during the last 70% of stride. However, due to the lack of knee flexion during the first single limb support peak (0-15% of stride) caused by the rigidity of the Mauch Microlite S knee, neither energy was harvested at the knee joint nor natural knee joint movement was obtained during the resistive flexion stage of gait moreover the required positive energy during push off was not obtained.

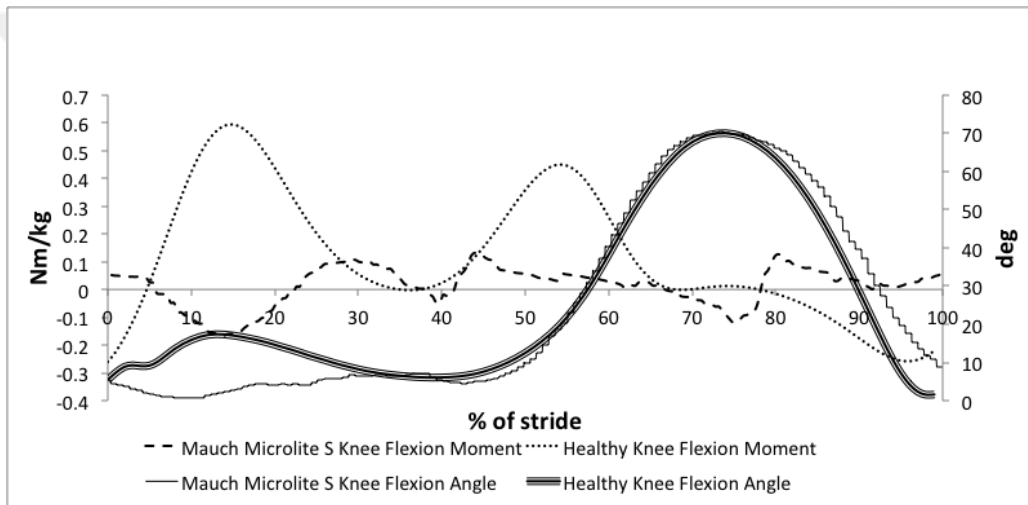


Figure 21: Symmetry of Gait during Normal Walking

The Mauch Microlite S knee was tested with a standard ankle joint, which was not capable of producing positive energy. Same procedure might provide closer to normal torque-angle properties, if the Mauch Microlite S knee is tested with a more sophisticated, energy regenerative ankle joint.

The modified trajectory, which provided the closest to normal GRF profile, may increase the probability of falls, reduce sense of balance and may not be replicated by an amputee. The purpose of the robotic simulation was to reproduce the hip movement until

the most desirable GRF profile, which would provide the closest to normal ground loading and desired propulsion, was achieved, thus maintaining the gait symmetry was not aimed. This work was justification for investigating the energy harvest capability of any prosthetic knee device by systematically modifying the hip joint biomechanics. Whereas the procedure to be followed should remain the same, the hip angle iteration should be done depending on the sophistication of both the tested prosthetic knee and the prosthetic foot, as more energy regenerative device would require less change in hip joint trajectory. Next study proposes an energy storage/release mechanism, which can be utilized in variable damping prosthetic knee devices so that an energy regenerative prosthetic knee can be tested and evaluated before starting the human testing.

CHAPTER V

VERIFICATION OF THE ENERGY HARVESTABLE TRANSFEMORAL PROSTHETIC KNEE

SPRING UNIT

5.1 Introduction

A Cleveland Clinic Foundation team has recently proposed a microprocessed prosthetic knee design, which is capable of harvesting and returning energy in a controlled way (van den Bogert et al., 2012). The hydraulic mechanism is composed of a rotary actuator and two accumulators and two valves (Figure 22). The actuator converts pressure to torque and torque to pressure. The high-pressure accumulator (HPA), which houses the spring, provides energy storage and release, while the low-pressure accumulator (LPA) houses the hydraulic fluid in the system.

During stance phase, as the patient weight creates pressure, hydraulic fluid flow is initiated through the HPA to obtain the required knee joint stiffness and store the available energy in the spring. When the applied weight starts to decrease, the accumulator pressure is routed back to the actuator to apply torque, which is needed to

flex the knee. The HPA and LPA valves open and close depending on the gait phase to permit hydraulic fluid flow from/to the actuator and regulate the spring compression/release. The electrical/electronic system includes the microprocessor and knee angle- force sensors, which send the real-time information to the microprocessor, to regulate the valves depending on the biomechanical demands of the performed activity.

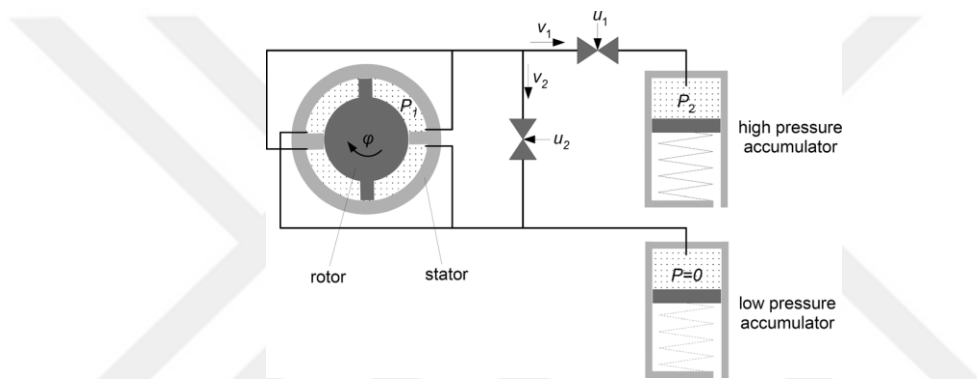


Figure 22: Mechanical schematic of the Cleveland Clinic Foundation Knee hydraulic system (adapted from van den Bogert et al., 2012)

During the first double limb support phase of the stride, body weight acts on the leg and initiates the knee flexion as well as the hydraulic fluid flow from the LPA to the HPA with the purpose of obtaining the desired knee joint stiffness and storing the available energy in the spring. Once the available energy is stored, the HPA valve closes and holds the pressurized fluid in the accumulator to maintain the spring compressed (Figure 23).

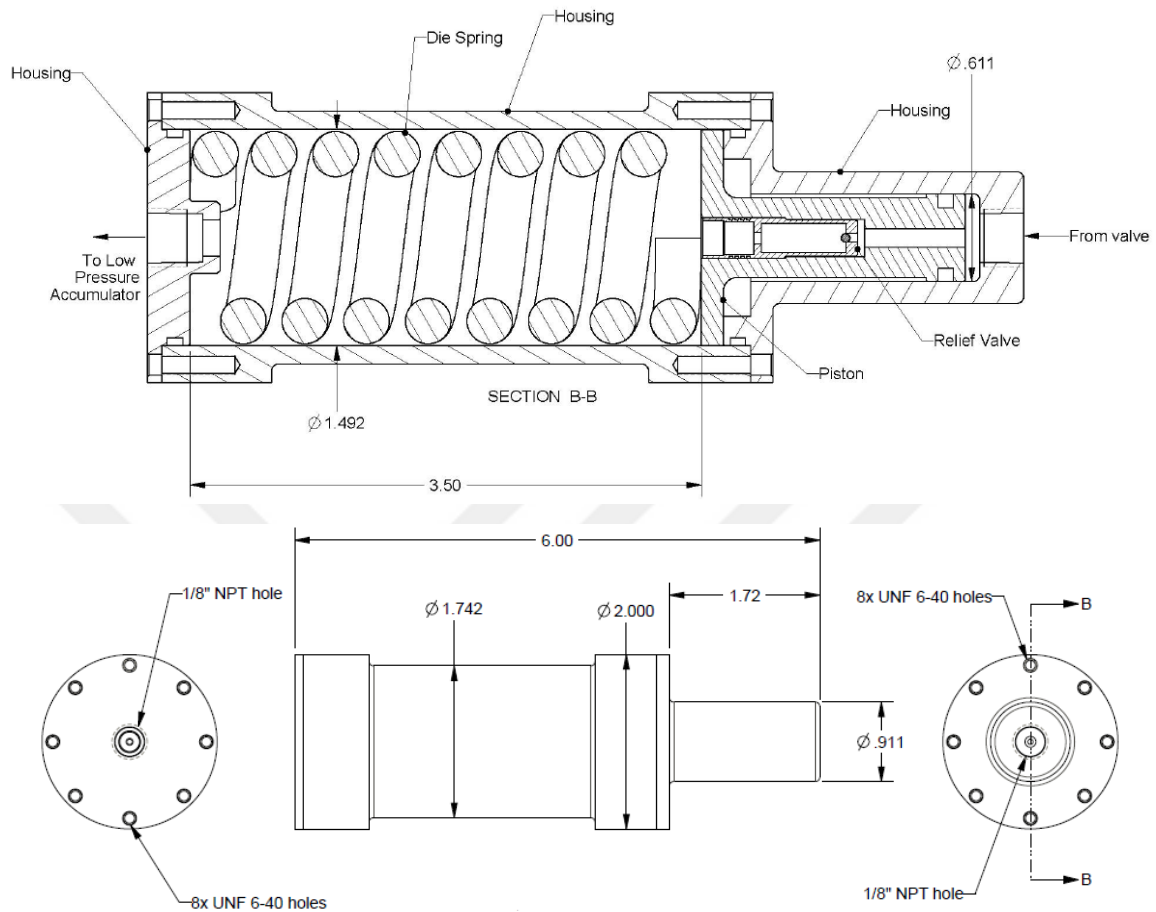


Figure 23: Schematics of the HPA and the Energy Storage Unit and HPA Components (all units in inches)

Orifice size modulation of the LPA valve provides the desired pressure/knee torque during the stance phase, where the body weight is carried by the prosthetic knee. For the duration of the late stance/early swing phases, LPA valve is closed and the HPA valve is opened to produce the needed torque in the actuator to initiate the knee flexion. Whereas the proposed design is still under development and the human testing results are not available in the literature yet, the optimal control simulation results during walking, running and sit/stand/sit sequence are presented recently (van den Bogert et al.,

2012). The results indicated that the proposed device provided near normal knee movement and stance phase flexion when the accumulator stiffness was adjusted to each tested activity.

5.1.1 Selection of the Energy Storage Unit

The variability in the desired functional stiffness values during the activities of daily living has been presented previously. The new generation prostheses utilize smart systems such as microprocessors, valves, pumps, motors etc. to supplement their pure mechanical components by instantaneously adjusting the amount and timing of the spring compression / release depending on the biomechanical demands of the performed activity (Sup et al., 2008; Martinez-Villalpando et al., 2009; van den Bogert et al., 2012). As it is not realistic to use different springs for different activities, the most effective solution would be obtaining variable stiffness with some hardware modifications, such as parallel oriented spring couplings, series of elastic actuators, pumps and valve couplings.

The lack of positive work harvest during the stance phase and appropriate knee flexion during the swing phase are the major drawback of the conventional prosthetics (Segal, 2006; Sup, 2008; Martinez-Villalpando, 2009), which causes the abnormal gait patterns and eventually amplifies the required metabolic power to complete the stride. Walking at variable cadence is a cyclic activity, which does not require a motor in order to provide the needed positive work to the knee joint (Winter, 1983; Sup, 2008; Martinez-Villalpando, 2009). In the proposed design, the efficiency and the high power-to-weight ratio of the spring is supplemented by a pair of accumulator-valve couplings, which

regulates the spring compression/ release by harvesting the available energy during the stance flexion phase and releasing it when the system requires positive energy. As the patient applies his/her body weight on the amputated side, the pressure is applied on the rotary actuator, which allows the rotor to turn and push the hydraulic fluid to the HPA depending on the instantaneous torsional stiffness (Figure 24).

In this study, knee joint torsional stiffness values were calculated during slow, normal and fast walking with the aim of selecting the favorable energy storage unit, which provides the best possible quantitative values during the stance flexion phases of these activities, when high change in the knee flexion moment and low change in the knee flexion angle present.

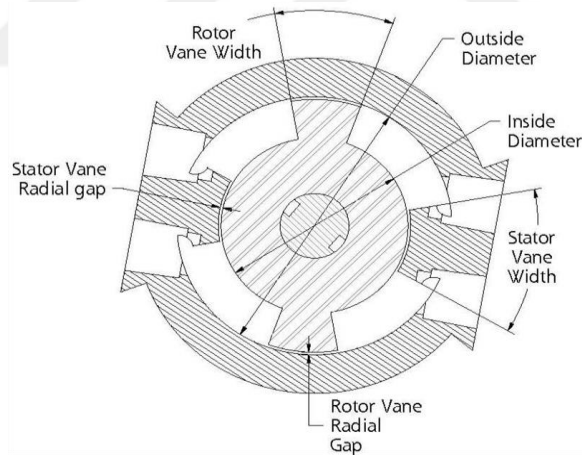


Figure 24: Rotary Actuator Schematics

Rotary actuator torsional stiffness (TS) was calculated according to the sagittal plane biomechanics of the 12 able-bodied subjects. The energy harvest periods for each activity, when the knee joint flexes and generates energy, were identified according to the sagittal plane knee joint power vs. % of stride curves (Figure 25).

$$TS = (DM / Da) * (180 / p)$$

where, ΔM indicates the sagittal plane knee joint flexion moment curve slope, $\Delta \alpha$ the sagittal plane knee joint flexion angle curve slope.



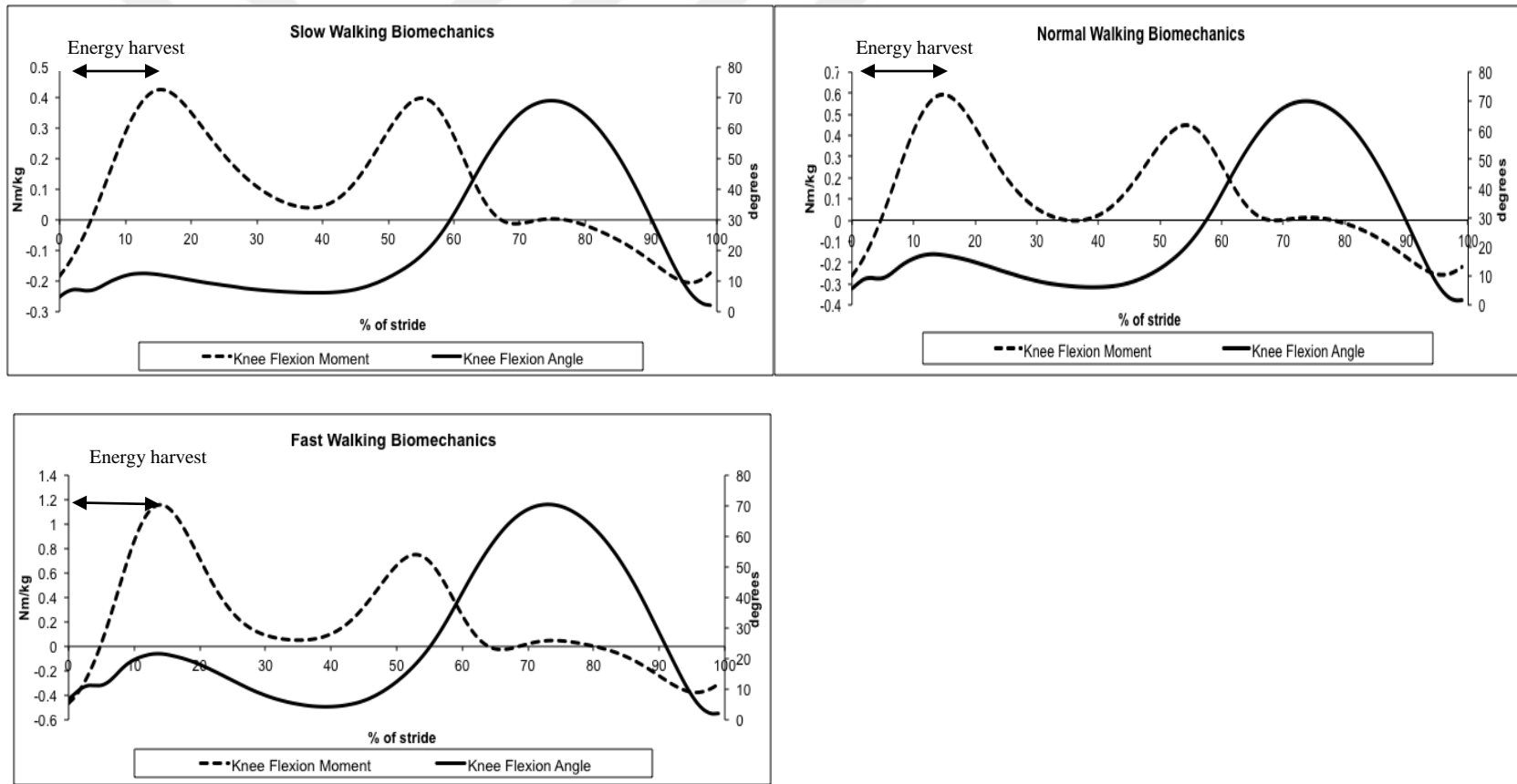


Figure 25: Slow (101.9 ± 7.3 steps/min), Normal (113.9 ± 7.6 steps/min), and Fast (125.3 ± 11.8 steps/min) cadences of the healthy knee joint: only the intervals where the amputated side carries the whole body weight (single limb support) were considered as the energy harvest periods. Participants: $n=12$, mean age: 30.42, SD: 4.87 yr; mean height: 1.71, SD: 0.049 m; mean mass: 70.8, SD: 15.9 kg, mean Body Mass Index: 23.9, SD: 2.99 kg/m².

$$\Delta M = P \times h \times (R^2 - r^2)$$

Where, P indicates the pressure drop at the rotary actuator, h the height of the fluid compartment, R^2 the stator radius and r^2 the rotor radius

$$V = A_p \times \Delta X$$

Where, V indicates the volume change in the HPA as a result of the applied pressure, A_p the HPA piston area and ΔX is the HPA piston displacement

$$k = F/\Delta X$$

Where F indicates the torque (flexion force) applied at the knee joint, ΔX the spring compression

$$k = (P \times A_p) / \left(\frac{V}{A_p}\right)$$

$$k = (\Delta M / (h \times (R^2 - r^2) \times A_p^2)) / (\Delta \alpha \times (h \times (R^2 - r^2)))$$

Where $\Delta \alpha$ indicates the change in knee flexion angle

$$k = TS \times (A_p / (h \times (R^2 - r^2)))^2$$

Specification	Value
Average Knee Joint Torsional Stiffness	37696 N cm/ rad
HPA Piston Area	1.885 cm ²
Height of the Fluid Compartment	0.762 cm
Stator Radius	2.540 cm

Rotor Radius	1.778 cm
Length of the Vane	2.540 cm
Energy Storage Unit Stiffness	1918.61 N/cm

Table iv: Design Specifications

Specification	Value
Outer Diameter	3.098 cm
Free Length	7.62 cm
Stiffness	2076 N/cm
Solid Length	5.689 cm

Table v: LHL 1250D 03 Spring Specifications (Lee Springs, Medium Load Series (www.leespring.com))

5.2 Methods

5.2.1 Verification Tests of the Energy Storage Unit

The purpose of the verification testing is to present the pressure vs. displacement relationship of the activities of daily living.

$$P = \left(\frac{M_{max}}{r}\right)/A$$

Where, r indicates the lever arm and A the area, where the pressure is applied

$$r = (d_i + h_v)/2$$

Where d_i indicates the rotor diameter and h_v the height of the fluid compartment

$$A = A_v \times n_i$$

Where A_v indicates the area of one vane and n_i the number of the fluid compartment

$$A_V = h_V \times l_V$$

Where, l_V indicates the length of the vane.

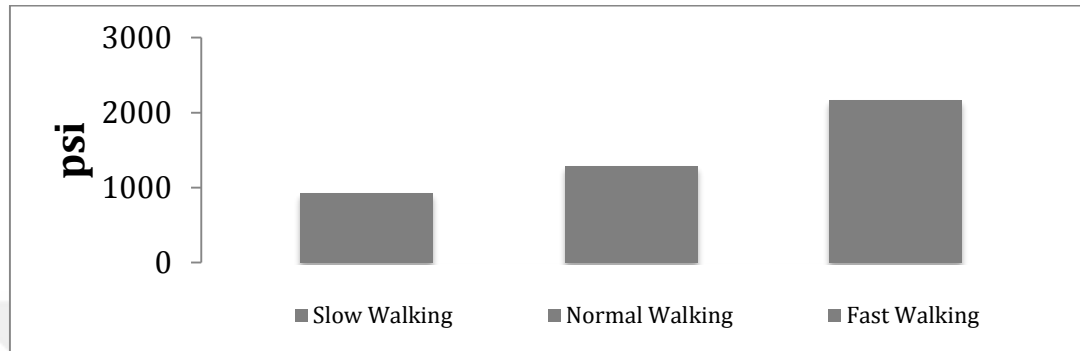


Figure 26: Maximum pressure applied at the knee joint during stance flexion phases of slow, normal and fast walking

In the verification testing, the HPA pressure vs. displaced volume relationship was determined theoretically (Figure 27). According to the calculated pressure values of the tested daily activities, 2200 psi was the maximum pressure applied at the HPA during the stance flexion phase of the stride (Figure 26). As long as the demands of the fast walking activity were satisfied, normal and slow walking demands were considered to be satisfied as well.

The displaced volume was calculated by;

$$V = l_s \times A_P$$

Where l_s indicates the stroke length, which was calculated by;

$$l_s = (P \times A_P) / k$$

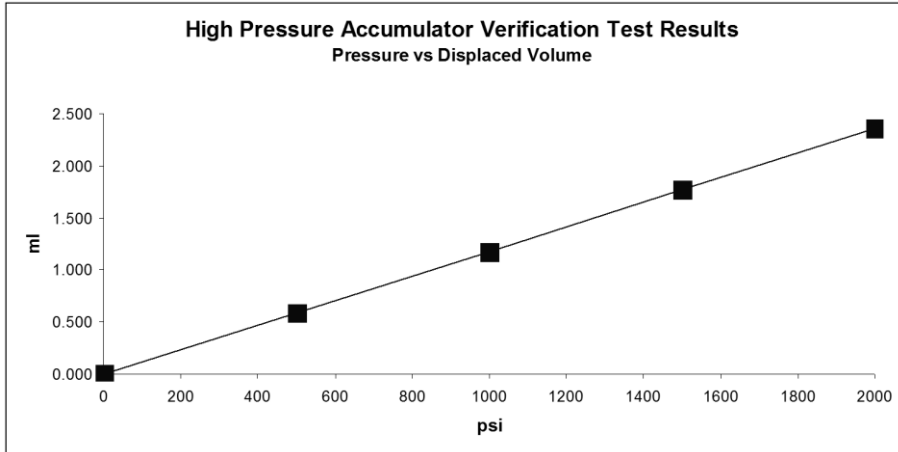


Figure 27: Verification Test Results of the HPA

5.2.2 Validation Tests of the Energy Storage Unit

Figure 28 shows the experimental setup for the HPA validation testing. The test spring was placed in the HPA through the body bottom and the bottom flange was screwed to the accumulator tightly in order to prevent hydraulic fluid leakage. The initial value, which the caliper showed while no pressure was applied to the HPA was recorded and called as “the relaxed spring caliper reading”. As the pressure was increased, obtained caliper readings were recorded and the differences between the relaxed spring caliper reading and the recorded values were calculated. The obtained deformation was used as the stroke length.



Figure 28: The High Pressure Accumulator and the caliper positioning

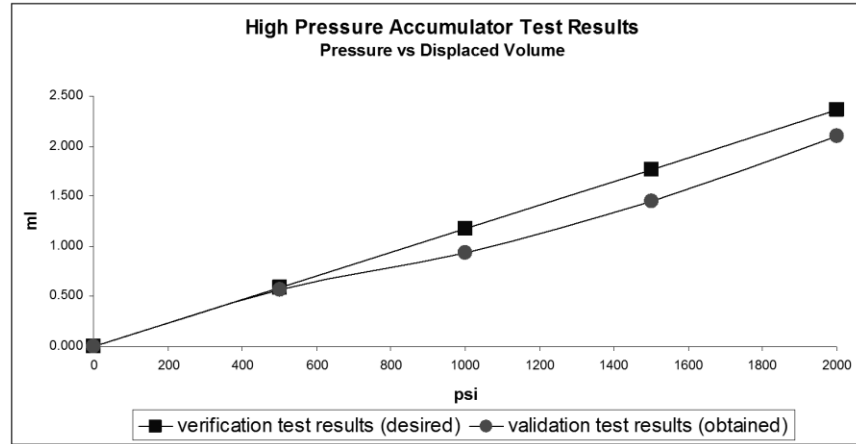


Figure 29: Validation Test Results of the HPA: strong positive correlation between the verification and validation test results has been established ($r= 0.9959$)

5.3 Conclusion

In designing transfemoral prostheses, which harvest energy from the movement of the user and instead of releasing it immediately, keep it until the energy is most needed during the swing phase is crucial for achieving assisted and energy regenerative ambulation. During the activities, which are not cyclic and either require net positive energy or do not have sequential positive and negative energy intervals throughout the gait cycle, a simple spring mechanism would be insufficient in achieving fully assisted and energy regenerative gait. Therefore, it is anticipated that, without a motor use or some hardware modifications, such as parallel oriented spring couplings and series of elastic actuators, transfemoral amputees would be performing the activities, which are not cyclic, either with a step-by-step technique where the healthy leg leads while the prosthetic limb follows it passively, or with asymmetrical posture and abnormal movement of the amputated side hip joint.

Conversely, according to the results of the verification and validation tests, a spring ($k=2076$ N/cm) and accompanying mechanical and electrically controlled mechanisms would be an effective way to control the spring compression and release with the purpose of obtaining the required knee joint stiffness during the tested cyclic activities of daily living, which do not require net positive energy. This study evaluated the energy storage unit performance during cyclic activities of daily living theoretically and experimentally (Figure 29). The strong correlation ($r=0.9959$) between the test results indicated that by using modern computational and simulation tools, a prosthetic knee device and its components could be designed and validated even before initiating the hardware design process and human testing.

CHAPTER VI

CONCLUSIONS AND FUTURE WORK

6.1 Conclusions

By using modern computational tools, a prosthetic knee device could be simulated even before initiating the hardware design process. The challenging aspect of a gait cycle is that, energy absorption does not always immediately follow energy generation, moreover the generated and absorbed energy amount quantities are not the same. This makes it essential to control energy throughout the gait cycle, by harvesting and storing energy, and releasing it when needed since even for the most energy efficient activity, walking at self-selected cadence, total negative work can be -34 J and positive work can be 50 J (DeVita et al., 2007). This makes control of power throughout the gait cycle potentially very useful.

Energy efficiency can be elevated through various energy generation and storing approaches during gait. One of them is to use a spring in the prosthesis. For storing and releasing energy during gait, springs have been used in many prosthetic devices. Since stride is a closed loop that has positive and negative work phases, using a spring cuts the power demand significantly. Instead of using heavy motors, gearbox and huge batteries

to feed them, a spring possibly might maintain the same performance with less weight. The issue is controlling the energy return to be effective in its timing and duration.

This work investigates the significance of energy flow at the knee joint by quantifying storage and release of energy at various phases of the gait cycle both for the healthy and a prosthetic knees. The energy harvest interval for a healthy and a prosthetic knee is not always the same because the healthy knee is supplemented by the ankle joint, which allows balanced energy distribution in the ankle and knee joints during a single stride. The ankle joint behaves as an energy generator during the pre-swing phase and stores up to 80% of the required energy (Unal et al. 2010) which is used as the missing positive energy at the knee joint during push off. However, a prosthetic knee cannot be supplemented by a fully energy regenerative ankle joint, which obliges the prosthetic knee to harvest energy during the loading response phase of gait, when the body weight is applied on the knee and the spring is compressed.

The purpose behind the spring use as the energy storage mechanism in prosthetic knee design is for replicating the brake (eccentric) behavior of the muscles of the knee joint, however, knee joint stiffness varies significantly during the activities of daily living. Exploring this variation is crucial for the design of transfemoral prosthetic devices that aim to mimic normal gait. The active knee joint functional stiffness during slow/normal/fast walking, slow running, stair ascent/descent and sit/stand/sit sequence were analyzed in order to present the favorable loading and unloading spring stiffness. With the same purpose, the significance of this work was demonstrated by testing a common commercially-available prosthetic leg (one that is purely passive) was tested

with a 3 DOF gait simulator – a system that allows the torque-angle properties of the knee joint to be evaluated. Moreover, the functional stiffness of an energy storage mechanism, which would provide the needed positive energy during the cyclic activities of daily living, was analyzed theoretically. Active healthy knee joint functional stiffness during slow (0.005 N/kg deg.)/normal (0.004 N/kg deg.) /fast (0.003 N/kg deg.) walking, slow running (0.052 N/kg deg.), stair ascent (0 N/kg deg.) /descent (0.012 N/kg deg.) and sit/stand/sit sequence (0.006 N/kg deg.) were determined. The average functional stiffness during loading (0.011 Nm/kg deg. (sd: 0.018)) and unloading (0.024 Nm/kg deg. (sd: 0.0128)) were investigated to guide the prosthetic knee developers during the design strategy determination period. With the same intention the functional stiffness of a purely passive Mauch Microlite S knee a purely passive prosthetic knee during normal walking by a 3 DOF gait simulator (0.0004 Nm/kg deg.) was analyzed and the obtained results were compared to the healthy knee joint functional stiffness during the resistive flexion (15% of stride- loading response) stage of gait.

This thesis presented the functional stiffness analysis of the knee joint clinically, theoretically and robotically with the aim of investigating its energy flow characteristics, therefore an energy regenerative prosthetic knee device could be designed and tested in terms of energy harvest/return properties, needed for providing the missing positive energy during push off. Therefore the findings of this work are crucial in understanding the healthy knee, its energy flow characteristics and the biomechanical demands of a prosthetic knee device in order to mimic the healthy knee. Therefore, by using modern

computational tools, a prosthetic knee device could be simulated even before initiating the hardware design process.

6.2 Future Work

The future research objectives aim to improve the functional stiffness analysis of the purely passive transfemoral prosthetic and healthy knees. In order to achieve this, active ankle joint functional stiffness during the activities of daily living need to be analyzed. Additionally, a purely passive prosthetic knee will be simulated with an energy regenerative ankle joint during more energy demanding activities and the gait symmetry will be compared with the able-bodied human biomechanics.

The future research objectives aim to improve the healthy knee joint functional stiffness analysis by investigating the ramp walking analysis. Also functional stiffness of the active ankle joint during the activities of daily living will be investigated in order to understand the energy flow at the ankle joint and design energy regenerative prostheses.

The role of the prosthetic foot selection in achieving more natural and energy regenerative gait will be evaluated by testing the Mauch Microlite S knee with a more sophisticated and energy regenerative ankle joint such as Össur Proprio Foot, which provides powered ankle motion and intelligent terrain adaptation. Additionally the Mauch Microlite S knee will be tested on an able-bodied subject by using a wearable adaptor and the simulation results will be compared the clinical data. The simulation of the Mauch Microlite S knee will be improved by investigating the other daily activities such as walking at various cadence, stair ascent/decent and walking on the ramp.

BIBLIOGRAPHY

- Adams, P.F., Hendershot, G.E., Marano, M.A. (1999). Current estimates from the National Health Interview Survey. National Center for Health Statistics. 10 (200)
- Aeyels, B.L., Peeraer, J., Sloten, V. (1992). Development of an above-knee prosthesis equipped with a microcomputer-controlled knee joint: First test results. *Journal of Biomedical Engineering*. 4 (11), 199-202.
- Alexander, R.M. (1991). Energy-saving mechanisms in walking and running. *Journal of Experimental Biology*. 160 (1), 55-59.
- Allcock, P. A., Jain, A. S. (2001). Revisiting transtibial amputation with the long posterior flap. *British Journal of Surgery*. 88, 683-686.
- Andriacchi, T.P., Ogle, J.A., Galante, J.O. (1977). Walking speed as a basis for normal and abnormal gait measurements. *Journal of Biomechanics*. 10 (1), 261-268.
- Argunsah, H., Davis, B.L. Application of Biomimetics in the Design of Medical Devices. In: Bar-Cohen, J. (eds.) *Biomimetics Nature-Based Innovation*. 1st ed. Florida, USA: CRC Press; 2012. p. 445-460
- Bechtol, C.O. The suction socket. *The journal of American medical association*. 1951; 146(7): 625-628
- Bedard, S., Roy, P. Actuated Leg Prosthesis for Above-Knee Amputees. United States patent 7314490. 2003
- Bogert, A.J. van den, and J.J. de Koning, Optimal filtering for inverse dynamics analysis. *Proc. 9th CSB Congress, Burnaby, B.C., 1996*. P 214-215.
- Braune, W., Fischer, O. Determination of the moments of inertia of the human body and its limbs. 1st ed. Berlin, Germany. Springer-Verlag; 1988

- Buckley, J.G., Jones, S.F., Birch, K.M. (2002). Oxygen consumption during ambulation: comparison of using a prosthesis fitted with and without a tele-torsion device. *Arch Phys Med Rehabil.* 9 (83), 576-581.
- Centers for Disease Control and Prevention. Underlying Cause-of-Death: Mortality Archives. : <http://wonder.cdc.gov/mortArchives.html> (accessed August 10, 2009).
- Chen, I.H., Kuo, K.N., Andriacchi, T.P. (1997). The influence of walking speed on mechanical joint power during gait. *Gait and Posture.* 6, 171-176.
- Chin, T., Machida, K., Sawamura, S., Shiba, R., Oyabu, H., Nagakura, Y. (2006). Comparison of Different Microprocessor Controlled Knee Joints on the Energy Consumption during Walking in Trans-Femoral Amputees: Intelligent Knee Prosthesis (IP) versus C-leg. *Prosthetics and Orthotics International.* 30, 73-80.
- Currier, J.H., Duda, J. L., Collier, J. P., Sperling, D. K., Currier, B.H., Kennedy, F. E. (1998). In Vitro Simulation of contact Fatigue Damage Found in UHMWPE Components of Knee Prostheses. *IMechE Journal of Engineering in Medicine.* 212, 293-302.
- Demšar, I., Supej, M., Vidrih, Z., Duhovnik, J. (2011). Development of Prosthetic Knee for Alpine Skiing. *Journal of Mechanical Engineering.* 57, 768-777.
- Detrembleur, C., Vanmarsenille, J.M., De Cuyper, F., Dierick, F. (2005). Relationship between energy cost, gait speed, vertical displacement of center of body mass and efficiency of pendulum-like mechanism in unilateral amputee gait. *Gait and Posture.* 2, 333-340.
- DeVita, P., Helseth, J., & Hortobagyi, T. (2007). Muscles do more positive than negative work in human locomotion. *Journal of Experimental Biology,* 210, 3361-3373.
- DiAngelo, D.J., Winter, D.A., Ghista, D.N., Newcombe, W.R. (1989). Performance assessment of the Terry Fox jogging prosthesis for above-knee amputees. *Journal of Biomechanics.*; 22(6): 543-558

Dillingham, T. R., Pezzin, L.E., Mackenzie, E. J. (2002). Limb amputation and limb deficiency: epidemiology and recent trends in the United States. *Southern Medical Journal*. 95(8): 875-883

Dunne, A. Össur Power Knee.

http://www.ele.uri.edu/courses/ele282/F08/AndrewDunne_1.pdf (accessed 03 January 2012).

Edelstein J. E. Prosthetic feet: state of the art. *Physical therapy*.1988; 68(12): 1874-1881

Endolite. Smart adaptive microprocessor knee.
<http://www.endolite.com/products/knees/smartAdaptive.php> (accessed 22 August 2011).

Ernesto, C., Martinez-Villalpando, S.M., Herr, H. (2009). Agonist-antagonist active knee prosthesis: A preliminary study in level-ground walking. *Journal of Rehabilitation Research and Development*. 46(3): 361-374

Farber, B., Jacobson, J.S. (1995). An above-knee prosthesis with a system of energy recovery: A technical note. *Journal of Rehabilitation Research and Development*. 32(4): 337-348

Feinglass, J., Brown, J. L., LaSasso, A., Sohn, M. W., Manheim, L. M., Shah, S. J., Pearce, W. H. (1999). Rates of lower-extremity amputation and arterial reconstruction in the United States, 1979 to 1996. *American J. of Public Health*. 89 (8), 1222-1227.

Fraunhofer Institute for Manufacturing Engineering and Automation, Stuttgart. Orthopaedics and motion systems (Accessed Dec. 2012)
http://ipa.fraunhofer.de/Orthopaedics_and_Motion_Systems.83.0.html?&L=2.

Gailey, R., Allen, K., Castles, J., Kucharik, J., Roeder, M. (2008). Review of secondary physical conditions associated with lower-limb amputation and long-term prosthesis use. *J Rehabil Res Dev*. 45 (1), 15-29.

- Grimes, D.L., Flowers, W.C., Donath, M. (1977). Feasibility of an Active Control Scheme for Above Knee Prosthesis. *ASME Journal of Biomechanical Engineering*. 99 (4), 215-221.
- Guess TM, Maletsky LP. (2003). Computational modeling of a dynamic knee simulator for prediction of joint loading. In: Soslowky LJ, editor. *ASME 2003 Summer Bioengineering Conference*. 859–60.
- Guess TM; Maletsky LP. (2005). Computational modelling of a total knee prosthetic loaded in a dynamic knee simulator. *Medical Engineering & Physics*, 27 (5), 357-67.
- Ham, R., Cotton, L. (1991). *Amputation: from Aetiology to Rehabilitation*. 1st ed. London. Chapman and Hall
- Hansen, A.H., Childress, D.S., Miff, S.C., Gard, S.A., Mesplay, K.P. (2004). The human ankle during walking: implications for design of biomimetic ankle prostheses. *Journal of Biomechanics*. 37: 1467-1474
- HCFA. United States Health Care Financing Administration's common procedure coding system. <http://www.springerlink.com/content/nr66126774p15410/fulltext.pdf> (accessed 31 July 2012).
- Herr, H. (2002). Prosthetic and orthotic limbs. *Journal of Rehabilitation Research and Development*. 39(3): 11-12
- Herr, H., Wilkenfeld, A. (2003). User-adaptive control of a magnetorheological prosthetic knee, *Industrial Robot*. *Industrial Robot: An International Journal*. 30(1): 42-55
- Hogan, N., (1984). Adaptive Control of Mechanical Impedance by Coactivation of Antagonist Muscles, *IEEE Transactions on Automatic Control*, 29 (8).
- James, K.B., System for controlling artificial knee joint action in an above knee prosthesis. United States Patent 5,383,939.1995
- Johansson, J.L., Sherill, D.M., Riley, P.O., Bonato, P., Herr, H. (2005). A clinical comparison of variable damping and mechanically passive prosthetic knee devices. *Am J Phys Med Rehabil*. 45.

- Johns, R., Wright, V., (1962). Relative importance of various tissues in joint stiffness. *Journal of Applied Physiology*, 17 (5), 824–828.
- Kahle, J.T., Highsmith, M.J., Hubbard, S.L. (2008). Comparison of nonmicroprocessor knee mechanism versus C-Leg on Prosthesis Evaluation Questionnaire, stumbles, falls, walking tests, stair descent, and knee preference. *Journal of Rehabilitation Research & Development*; 45(1): 1-14
- Kastner, J., Nimmervoll, R., Kristen, H., Wagner, P. (1999). What are the benefits of the C-Leg? A comparative gait analysis of the C-Leg, the 3R45 and the 3R80 prosthetic knee joints. *Med Orthop Technol*; 119, 131-137
- Kirker, S., Keymer, S., Talbot, J., Lachmann, S. (1996). An assessment of the intelligent knee prosthesis. *Clinical rehabilitation*; 10: 267-273
- Kitayama, I., Nakagawa, N., Amemori, K. A, (1992). Microcomputer controlled intelligent A/K prosthesis. 7th World Congress of the International Society for Prosthetics and Orthotics.
- Klute, G.K., Berge, J.S., Orendurff, M.S., Williams, R.M., Czerniecki, J.M. (2006). Prosthetic Intervention Effects on Activity of Lower-Extremity Amputees. *Arch Phys Med Rehabil*. 87: 717-722
- Kulkarni J., Gaine W.J., Buckley J.G., Rankine J.J., Adams J. (2005). Chronic low back pain in traumatic lower limb amputees. *Clinical rehabilitation*; 19(1): 81-86
- Kulkarni, J. Letter to editor: post amputation syndrome. *Prosthetics and Orthotics International*.2008; 32(4): 434-437
- Kuo, A. D., (2007), The Six Determinants of Gait and the Inverted Pendulum Analogy: A Dynamic Walking Perspective, *Human Movement Science*, 26(4), 617–656.
- Laferrier, J.Z., Gailey, R. (2010). Advances in Lower-limb Prosthetic Technology. *Phys Med Rehabil Clinics of N. Am*; 87(21), 87-110

- Maletsky LP, Hillberry BM. (2000). Loading evaluation of knee joint during walking using the next generation knee simulator. In: Conway TA, editor. ASME Advances In Bioengineering, 48, 91–92.
- Mansour, J.M., Audu, M.L. (1986). The passive elastic moment at the knee and its influence on human gait. *Journal of Biomechanics*. 19 (5), 369-373.
- Marks L.J., Michael J.W. (2001). Science, medicine and the future: Artificial Limbs. *British Medical Journal*. 323 (1), 732-735.
- Martin C. W. Otto Bock C-leg®: A review of its effectiveness. <http://www.crd.york.ac.uk> (accessed 31 August 11)
- Martinez-Villalpando, E.C., Herr, H. (2009). Agonist-antagonist Active Knee Prosthesis: A preliminary Study in Level-ground Walking. *Journal of Rehabilitation Research and Development*. 46 (3), 361-374.
- Mauch, H.A., Hydraulic control unit for prosthetic leg, United States Patent 2,859,451, 1956
- Michael, J.W. (1999) Modern prosthetic knee mechanisms. *Clin Orthop Relat Res*; 361:39-47
- Modan M, Peles E, Halkin H, Nitzan H, Azaria M, Gitel S, Dolfen D, Modan B. (1998). Increased cardiovascular disease mortality rates in traumatic lower limb amputees. *Am J Cardiol*. 82 (10), 1242-1247.
- Morrison, J.B. (1970). The Mechanics of Muscle Function in Locomotion. *Journal of Biomechanics*.3: 431-451
- Murray, M.P., (1967). "Gait as a total pattern of movement", *Am. J. Phys. Med*. 46, 290-333
- Norton, K.M. A brief history of prosthetics. In motion. <http://www.amputee-coalition.org/inmotion> (accessed December 2007).

- Olney, S.J., Griffin, M.P., McBride, I.D. (1994). Temporal, kinematic, and kinetic variables related to gait speed in subjects with hemiplegia: a regression approach. *Physical therapy*. 74:872-885
- Össur Flex Foot Asure (Accessed Jan. 2013) <http://www.Össur.com>
- Össur. Power Knee. 31. <http://bionics.Össur.com/Products/POWERKNEE/> (accessed 31 July 2012).
- Össur. Rheo knee. <http://www.Össur.com/pageid=12702> (accessed 23 September 2011).
- Otto Bock Orthopadische Industrie. C-LEG A new dimension in amputee mobility. <http://www.ottobockknees.com/knee-family/c-leg-microprocessor-prosthetic-knee/> (accessed 04 June 2012).
- Paul, J.P. (1971). Comparison of EMG Signals from Leg Muscles with the Corresponding Force Actions Calculated from Walk path Measurement. *Proceedings of the Conference on Human Locomotor Engineering*. 13-28
- Paul, J.P. (1966). The Biomechanics of the Hip-Joint and its clinical Relevance. *Proceedings of the Royal Society of Medicine*. 59(10): 943-948
- Pfeifer, S, Hardegger, M, Vallery, H, List, R, Foresti, M, Reiner, R, Perreault, J., (2011) Model-Based Estimation of Active Knee Stiffness, *IEEE International Conference on Rehabilitation Robotics*, 978-1-4244-9862-8/11
- Rubin, G. (1983). S-N-S Knees and the Bilateral A/K Amputee. *Clinical Prosthetics & Orthotics*; 7(4)
- Saunders J. B., Dec. M., Inman V. T., Eberhart H. D. (1953). The major determinants in normal and pathological gait. *The journal of bone & joint surgery*. 35:543-558
- Schaffer E., Kort C., Kreuter, P. The prosthetic knee: microprocessor and non-microprocessor knee joints. http://www.amputee-coalition.org/inmotion/nov_dec_08/prosthetic_knees.html (accessed 03 January 2010).

- Schmalz, T., Blumentritt, S., Jarasch R. (2002). Energy expenditure and biomechanical characteristics of lower limb amputee gait: the influence of prosthetic alignment and different prosthetic components. *Gait and Posture*. 16 (3), 255-263.
- Segal, A.D., Orendurff, M.S. (2006). Kinematic and kinetic comparisons of transfemoral amputee gait using C-Leg and Mauch SNS prosthetic knees. *Journal of Rehabilitation Research and Development*. 43(7): 857-870
- Silder, A, Whittington, B, Heiderscheit, B, Thelen, DG, (2006). Identification of passive elastic joint moment–angle relationships in the lower extremity. *Journal of Biomechanics* 40 (2007) 2628–2635
- Stein, J.L., Flowers, W. C. (1987). Stance Phase Control of Above-Knee Prostheses: Knee control versus SACH Foot Design. *Journal of Biomechanics*; 20(1): 19-28
- Stewart, C. P.U., Jain, A. S. (1993). 25 years of a total amputee service. *Prosthetics and Orthotics International*; 17:14-20
- Struyf, P. A., van Heugten, C. M., Hitters, M. W., and Smeets, R. J., (2009). The Prevalence of Osteoarthritis of the Intact Hip and Knee among Traumatic Leg Amputees. *Arch. Phys. Med. Rehabil.*, 90(3), 440–446.
- Su, P.F., Gard, S. A., Lipschutz, R. D., Kuiken, T. A. (2007). Gait characteristics of persons with bilateral transtibial amputations. *Journal Of Rehabilitation Research And Development*. 44(4): 491-501
- Sup, F, Varol, HA, Mitchell, J, Withrow, T, Goldfarb, M, (2008). Design and Control of an Active Electircal Knee and Ankle Prosthesis, *Proceedings of the 2nd Biennial IEEE/RAS-EMBS International Conference on Biomedical Robotics and Biomechatronics* Scottsdale, AZ, USA
- Teixeira, LF., Nadeau, S., Milot, M., Gravel, D., Requiiao, LF. (2008). Effects of cadence on energy generation and absorption at lower extremity joints during gait. *Clinical Biomechanics*, 23, 769-778

- Torburn, L., Powers, C.M., Guitierrez, R., Perry J. (1995). Energy expenditure during ambulation in dysvascular and traumatic below-knee amputees: a comparison of five prosthetic feet. *J Rehabil Res Dev*; 32:111-119
- U.S. Centers for Disease Control and Prevention. 2011 Diabetes National Fact Sheet. <http://apps.nccd.cdc.gov/DDTSTRS/FactSheet.aspx> (accessed 21 January 2011).
- Unal, R, Behrens, SM, Carloni, R, Hekman, EEG, Stramigioli, S, Koopman, HFJM, Prototype Design and Realization of an Innovative Energy Efficient Transfemoral Prosthesis, Proceedings of the 210 3rd IEEE RAS & EMBS International Conference on Biomedical Robotics and Biomechatronics, The University of Tokyo, 2010
- van den Bogert, T, Samorezov, S, Davis, B.L., Smith, W.A., (2012). Modeling and Optimal Control of an Energy-Storing Prosthetic Knee, *Journal of Biomechanical Engineering*, Vol. 134
- Vanderwerker E. (1976). A brief review of the history of amputations and prosthesis. *Inter clinic information bulletin*; 15(5): 15-16
- Varol, H.A., Sup, F., Goldfarb, M. (2008). Real-time Gait Mode Intent Recognition of a Powered Knee and Ankle Prosthesis for Standing and Walking. Proceedings of the 2nd Biennial IEEE/RAS-EMBS International Conference on Biomedical Robotics and Biomechatronics
- Vitali, M., & Robinson, K. P. (1987). *Amputations and Prostheses* (2nd Revised edition ed.)
- Walker, P. S., Blunn, G. W. and Lilley, P. A. (1996). Wear testing of materials and surfaces for total knee replacement. *J. Biomed. Mater. Res.*, 33, 159
- Waters R.L., Perry, J., Antonelli D., Hislop H. (1976). Energy Cost of Walking of Amputee: the Influence of Level of Amputation. *The journal of bone & joint surgery*. 42-46
- Waters, R.L., Yakura, J.S. (1989). The energy expenditure of normal and pathological gait. *Crit Rev Phys Rehabil Med*;1: 183-209

- Whittington, B, Silder, A, Heiderscheilt, B, Thelen, DG, (2008). The contribution of passive-elastic mechanisms to lower extremity joint kinetics during human walking. *Gait & Posture*, 27 (4), 628–634
- Whittle, M.W. *An Introduction to Gait Analysis*. 4th ed. Stoneham, Maryland, USA. Butterworth-Heinemann; 2007
- Wiest, J. What is new in prosthetic knees? <http://www.prostheticsinmotion.com/> (accessed 20 April 2012).
- Winter, D.A., (1983). Energy generation and absorption at the ankle and knee during fast, natural, and slow cadences. *Clinical Orthopaedics and Related Research*, 175, 147–154
- Winter, D.A., Robertson, D.G. (1978). Joint torque and energy patterns in normal gait. *Biol Cybern*; 29(3): 137-142
- Winters, J. Stark, L., Seif-Naraghi, A.H., (1988). An analysis of the sources of musculoskeletal system impedance, *Journal of Biomechanics*, 21 (12), 1011 – 1025
- Yoon, Y.S., Mansou, M., (1982). The passive elastic moment at the hip. *Journal of Biomechanics* 15, (1), 905–910
- Zhang, L.Q., Nuber, G, Butler, J, Bowen, M, Rymer, W.Z. (1998). In vivo human knee joint dynamic properties as functions of muscle contraction and joint position, *Journal of Biomechanics*, 31(1), 71 – 76
- Zissimopoulos, A., Fatone, S., and Gard, S. A., (2007), Biomechanical and Energetic Effects of a Stance-Control Orthotic Knee Joint, *J. Rehabil. Res. Dev.*, 44(4), 503.



APPENDIX

APPENDIX A

Test Circuit and Instrumentation

Test Elements:

- 1.** High Pressure Pump: Fenner Stone Inc. Hydraulic Pressure Regulator (9474T13), 0-3000 psi range
- 2.** Pressure Gage: Arrow Pneumatics, BG 9052TV-10 ¼ T IN-LINE FILTER-VTN-10M, 0-3000 psi range
- 3.** Digital Caliper: MITUTOYO Digital Caliper, Part # 73K0564, Absolute Digimatic, Measuring Range Max: 6", Accuracy: 0.001"
- 4.** HPA Body: designed at Cleveland Clinic, PN 11146
- 5.** HPA Up Flange: designed at Cleveland Clinic, PN 11144
- 6.** HPA Bottom Flange: designed at Cleveland Clinic, PN 11145
- 7.** HPA Piston: designed at Cleveland Clinic, PN 11152-2
- 8.** HPA Piston Roll Pin: designed at Cleveland Clinic, PN 11152-6
- 9.** HPA Piston Seal: designed at Cleveland Clinic, PN 11152-5
- 10.** HPA Piston Upper Sleeve: designed at Cleveland Clinic, PN 11152-4
- 11.** HPA Piston Lower Sleeve: designed at Cleveland Clinic, PN 11152-3
- 12.** Energy Storage Unit: LHL 1250D 03, Lee Springs (www.leespring.com), Hefty Springs, Medium Load Series.
- 13.** Test Fluid: Hydraulic fluid, multi-purpose machine oil 46 198-235 SUS @ 100° F, SAE 10

APPENDIX B HPA Test Protocol

1. The placement of the HPA is chosen such that the caliper can be placed into the accumulator thru the spring for deflection measurements
2. Disassemble the bottom flange of the accumulator
3. Place the spring into the HPA through the bottom flange
4. Screw the bottom flange to the HPA
5. Apply 200 psi pressure to the HPA and fill it with hydraulic fluid
6. Keep applying pressure until fluid comes out from the top flange and make sure that all the air inside of the HPA is removed
7. Check the tightness of the screws

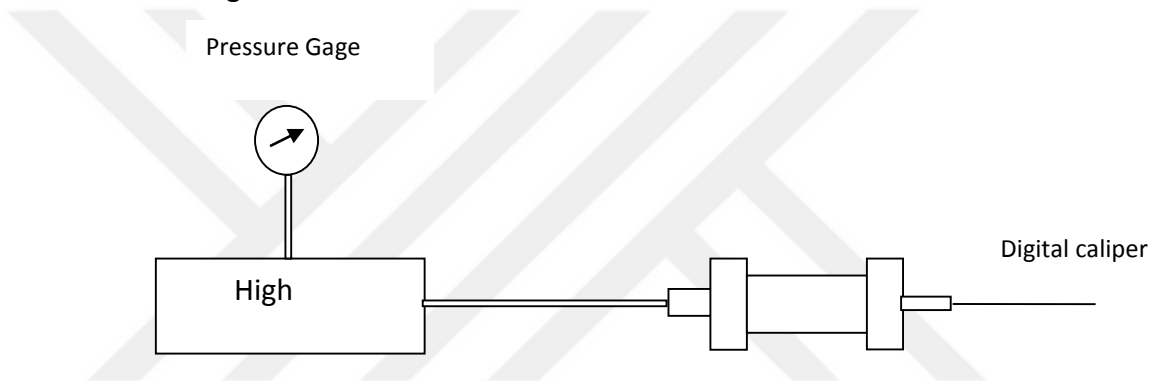


Figure 1: High Pressure Accumulator Test Configuration

8. Apply 2000 psi pressure to the HPA and make sure that there is no leakage
9. Calibrate the digital caliper
10. Push the caliper inside of the HPA through the bottom flange
11. Make sure that the caliper and the HPA are parallel
12. Record the relaxed spring caliper reading value as the reference value
13. Apply 500 psi pressure to the HPA
14. Record the caliper reading
15. Increase the pressure to 1000 psi
16. Record the caliper reading
17. Increase the pressure to 1500 psi
18. Record the caliper reading
19. Increase the pressure to 2000 psi
20. Record the caliper reading
21. During taking measurements make sure that the caliper moves freely without any distraction
22. Calculate the deformation value for each pressure rate by subtracting the caliper reading from the relaxed spring caliper reading

APPENDIX C
HPA Spring Alternatives and Test Results



Figure 1: Test Springs with and without the inserts (LHL 1000D 05, LHL 1250D 03, LHL 1500D 01) www.leespring.com, Hefty Springs, Medium Load Series

	LHL 1000D 05 (Spring 1)	LHL 1250D 03 (Spring 2)	LHL 1500D 01 (Spring 3)
Outer Diameter (cm)	2.5	3.1	3.7
Free Length (cm)	8.9	7.6	5.1
Rate (N/cm)	1024.5	2076	3861.4
Solid Length (cm)	6.3	5.7	3.8

Table 1: Test Spring Specifications

**Spring 1 w/o
metal insert**

Pressure (psi)	Deformation (in)	Displaced Volume (in ³)	Displaced Volume (ml)	Compliance ($\Delta V/\Delta P$)
500	0.07	0.13	2.05	4.11E-03
1000	0.14	0.24	3.96	3.96E-03
1500	0.20	0.35	5.77	3.84E-03
2000	0.26	0.45	7.39	3.70E-03

**Spring 1 w
metal insert**

Pressure (psi)	Deformation (in)	Displaced Volume (in ³)	Displaced Volume (ml)	Compliance ($\Delta V/\Delta P$)
500	0.07	0.12	2.03	4.07E-03
1000	0.14	0.24	3.87	3.87E-03
1500	0.20	0.34	5.64	3.76E-03
2000	0.24	0.43	7.00	3.20E-03

**Spring 2 w/o
metal insert**

Pressure (psi)	Deformation (in)	Displaced Volume (in ³)	Displaced Volume (ml)	Compliance ($\Delta V/\Delta P$)
500	0.12	0.21	3.40	6.81E-03
1000	0.19	0.34	5.58	5.58E-03
1500	0.30	0.53	8.65	5.76E-03
2000	0.44	0.77	12.55	6.28E-03

Spring 2 w metal insert

Pressure (psi)	Deformation (in)	Displaced Volume (in ³)	Displaced Volume (ml)	Compliance ($\Delta V/\Delta P$)
500	0.01	0.03	0.43	8.59E-04
1000	0.12	0.22	3.52	3.52E-03
1500	0.16	0.28	4.67	3.11E-03

Spring 3 w/o metal insert

Pressure (psi)	Deformation (in)	Displaced Volume (in ³)	Displaced Volume (ml)	Compliance ($\Delta V/\Delta P$)
500	0.26	0.45	7.42	1.48E-02
1000	0.45	0.78	12.75	1.27E-02
1500	0.66	1.16	18.97	1.26E-02
2000	0.85	1.49	24.47	1.22E-02

Table 2: Test Results: Pressure vs. Displaced Volume

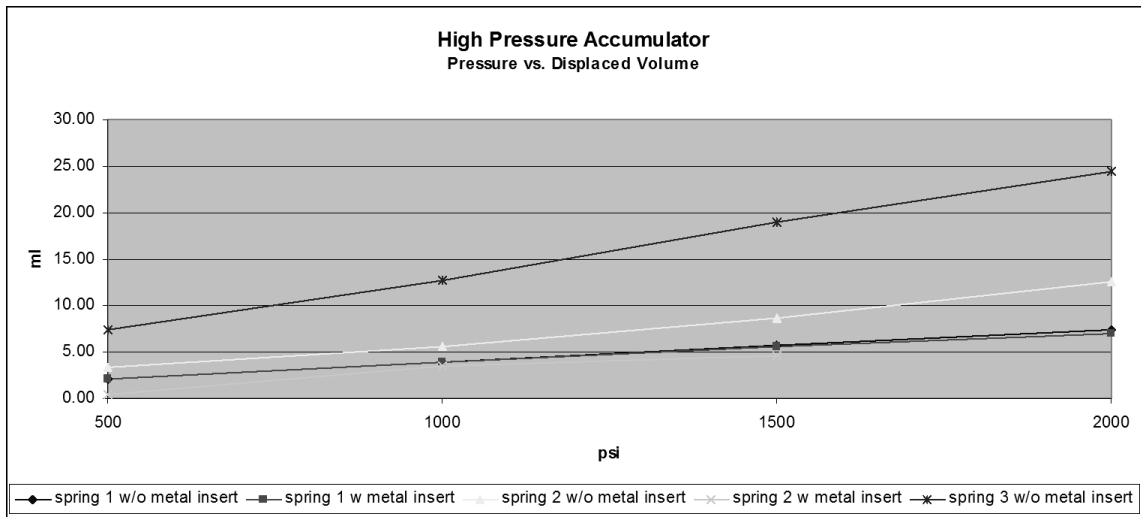


Figure 2: Pressure vs. Displaced Volume at High Pressure Accumulator

APPENDIX D

Abbreviations

DOF: Degrees of Freedom

GRF: Ground Reaction Force

APM: Artificial Proprioception Module

SNS: Stance and Swing

BMI: Body Mass Index

HPA: High Pressure Accumulator

LPA: Low Pressure Accumulator

TS: Torsional Stiffness

